Symposium on Positron Emission Tomography

September 19th - 22nd 2013, Jagiellonian University, Kraków, Poland

RPC-PET
Positron Emission Tomography
with
Resistive Plate Chambers

(off-road PET wanderings)

P. Fonte

LIP-Coimbra

The RPC-PET team

Researchers and engineers				*Technicians*	
Name	**Institute**	**Name**	**Institute**	**Name**	**Institute**
Adriano Rodrigues	ICNAS/FMUC	Luís Mendes	FMUC	Americo Pereira	LIP
Alberto Blanco	LIP	M. Kajetanowicz	NE	Carlos Silva	LIP
Antero Abrunhosa	ICNAS	Marek Palka	JU	João Silva	LIP
Carlos Silvestre	ISEC	Michael Traxler	GSI	Joaquim Oliveira	LIP
Custódio Loureiro	FCTUC	Miguel Couceiro	LIP/ISEC/FCTUC	Nuno Carolino	LIP
Durval Costa	HPP	Miguel Oliveira	LIP	Ricardo Caeiro	LIP
Filomena Clemêncio	FCTUC	Nuno Chichorro	ICNAS/FMUC		
Francisco Caramelo	FMUC	Orlando Oliveira	LIP		
Grzegorz Korcyl	JU	Paulo Crespo	LIP		
Isabel Prata	IBILI	Paulo Fonte	LIP/ISEC		
Jan Michel	IKF	Paulo Martins	LIP		
J.J. Pedroso Lima	LIP	Rui Alves	LIP		
Jorge Landeck	FCTUC	Rui F. Marques	LIP/FCTUC		

FCTUC: Departamento de Física da Faculdade de Ciências e Tecnologia da Universidade de Coimbra.
FMUC: Faculdade de Medicina da Universidade de Coimbra.
GSI: Helmholtz Centre for Heavy Ion Research, Darmstadt, Germany
HPP: Hospitais Privados do Porto, Porto, Portugal
IBILI: Instituto Biomédico de Investigação da Luz e Imagem da Faculdade de Medicina da Universidade de Coimbra.
ICNAS: Instituto de Ciências Nucleares Aplicadas à Saude da Universidade de Coimbra, Coimbra, Portugal.
IKF: Institut für Kernphysik, Goethe-Universität, Frankfurt, Germany
ISEC: Instituto Superior de Engenharia de Coimbra, Coimbra, Portugal.
JU: Jagiellonian University of Cracow, Cracow, Poland.
LIP: Laboratório de Instrumentação e Física Experimental de Partículas, Coimbra, Portugal.
NE: Nowoczesna Elektronika, Crakow, Poland

Past collaborators

C.M.B.A. Correia[2], L. Fazendeiro[1], M.F. Ferreira Marques[4,5], C. Gil[4], M. P. Macedo[2,5]

1 LIP, Laboratório de Instrumentação e Física Experimental de Partículas, 3004-516 Coimbra, Portugal.
2 CEI, Centro de Electrónica e Instrumentação, Univ. Coimbra, 3004-516 Coimbra, Portugal.
4 ICEMS, Departamento de Física, Universidade de Coimbra, 3004-516 Coimbra, Portugal.
5 ISEC, Instituto Superior de Engenharia de Coimbra, 3031-199 Coimbra, Portugal

Principles of PET

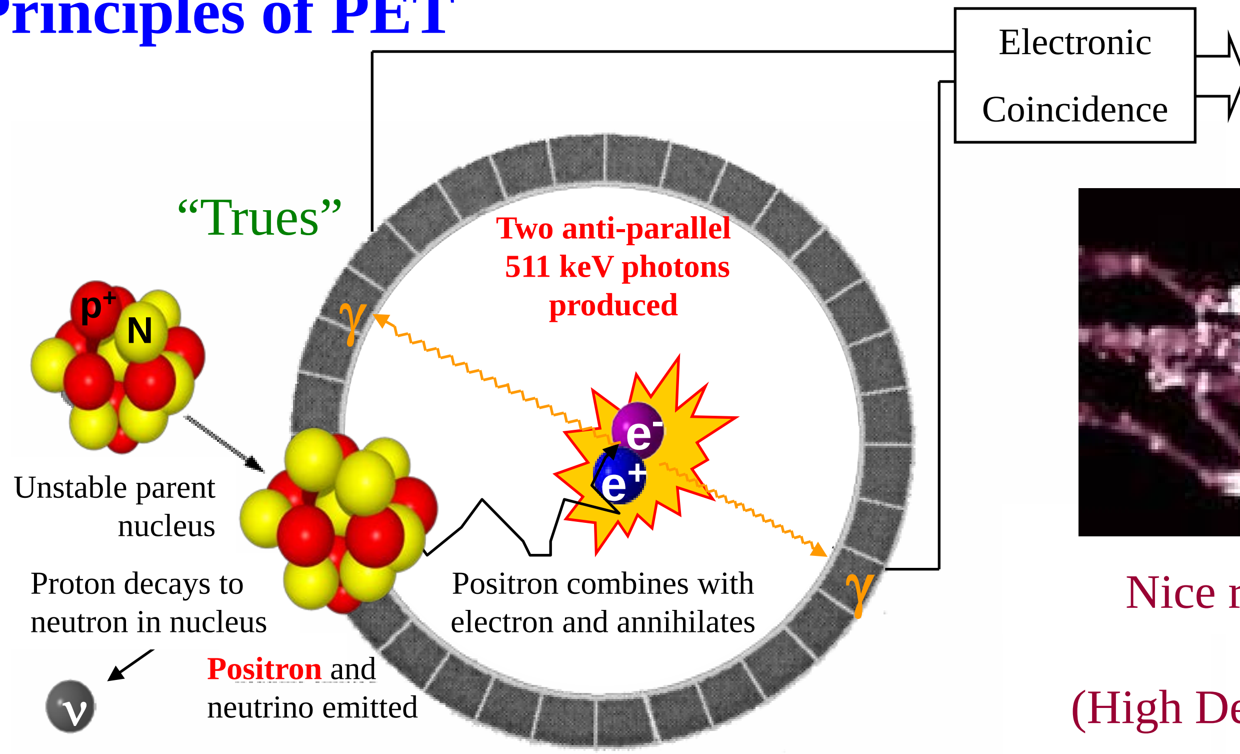

Time coincidence is the main trigger

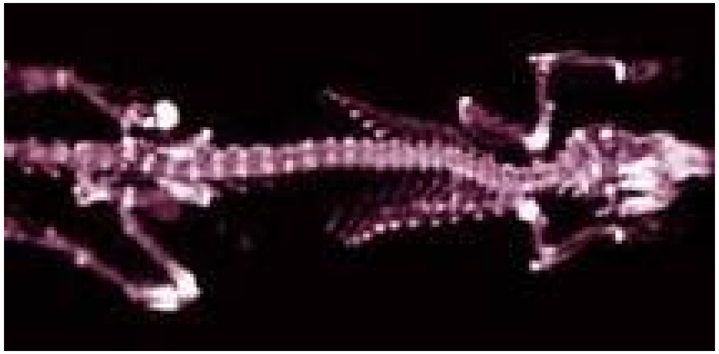

Nice rat image taken with the "HIDAC" scanner
(High Density Avalanche Chamber)

Sources of image noise (background):

$$NEC = \frac{T^2}{T + S + 2R}$$

Counting noise

"Randoms"

Avoided by sharper timing

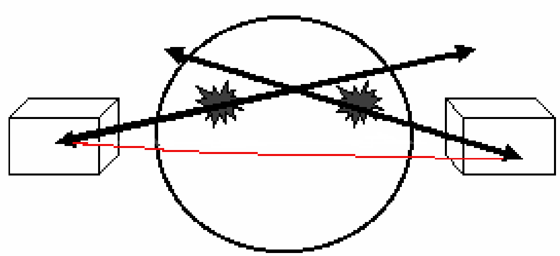

"Scatters"

Avoided by energy discrimination

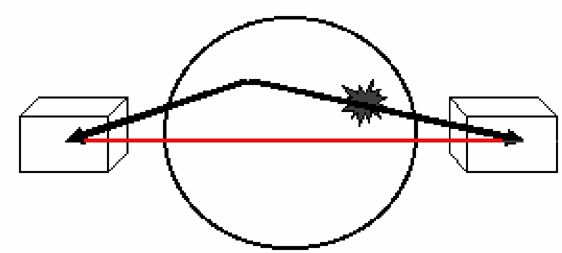

TOF (time-of-flight) - PET

$$TOF\ sensitivity\ advantage \approx \frac{object\ size}{\underbrace{(c/2)\ time\ resolution}}$$

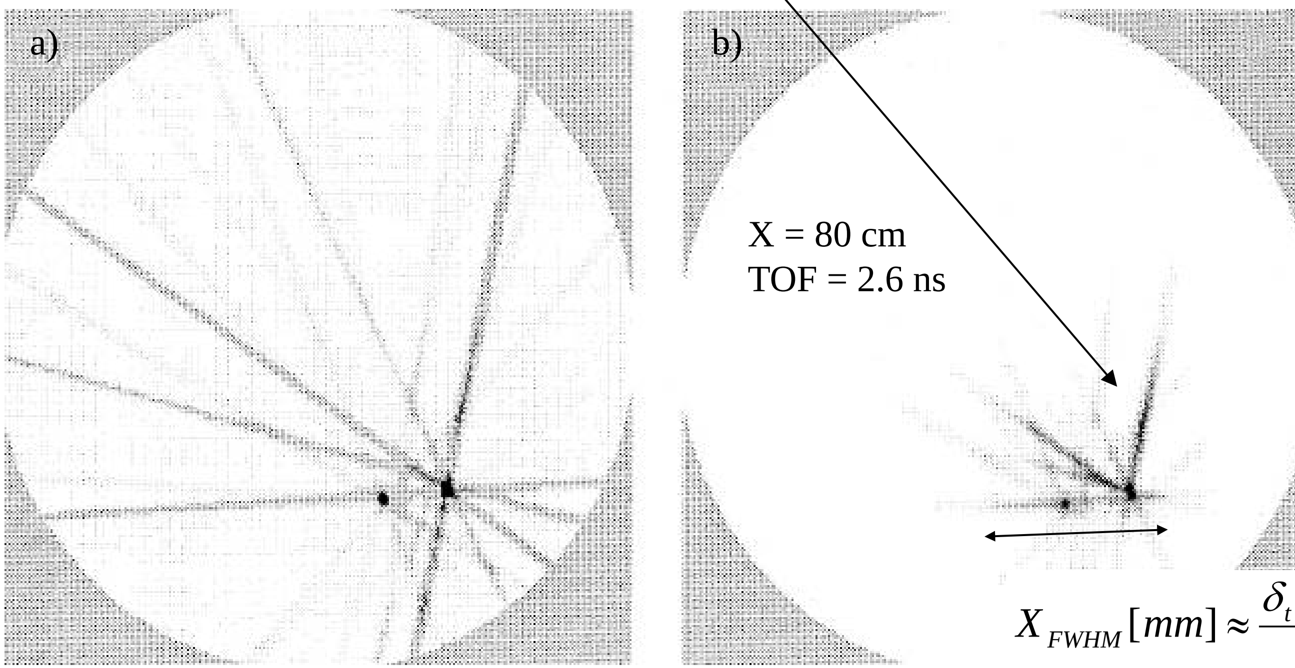

$$X_{FWHM}[mm] \approx \frac{\delta_t[ps]}{2}$$

a) Reconstructed image without TOF.
b) Reconstructed image using TOF information

[NIM A 471(2001) 200-204]

Single-bed full-body human PET

Standard PET

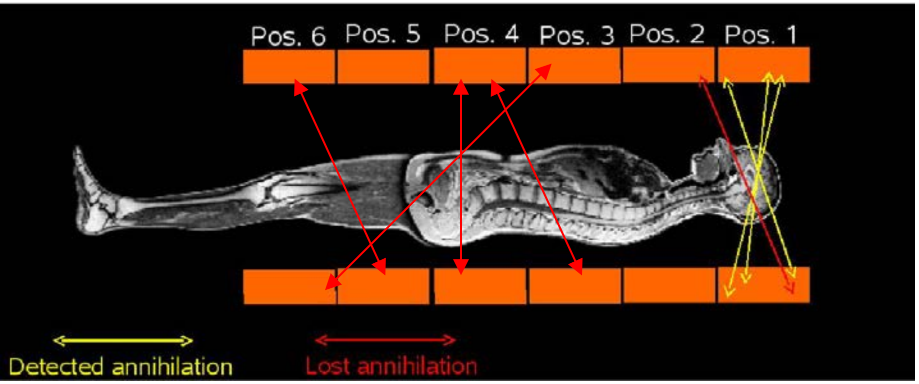

Most photons are lost

Whole-body FOV PET

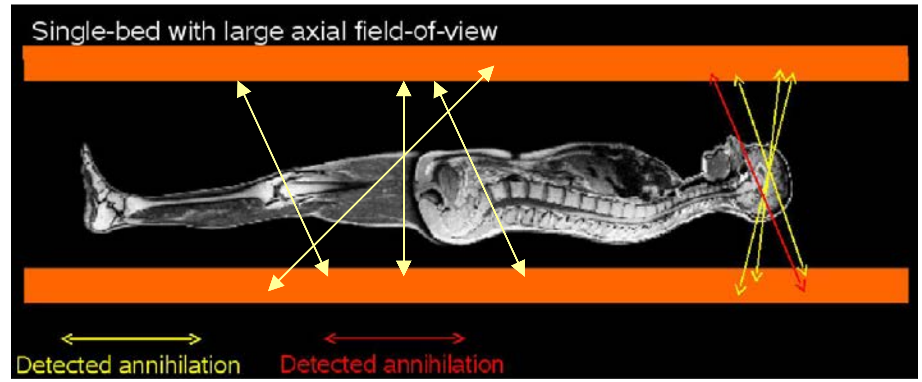

2.4 m

Most photons have a chance to be seen

[D.B.Crosetto 2000 IEEE NSS]

Made with crystal “blocks” 5x5 cm

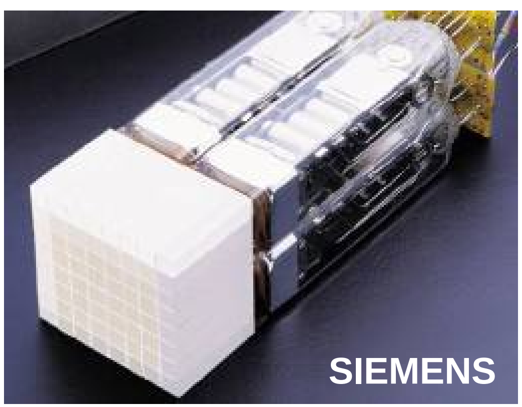

Comercial value=1.5M€

Extremely expensive if based on crystals
⇒ RPC-PET

The concept was independently reviewed by mainstream workers and found worth pursuing.

[L.Erickson et al, 2008 IEEE MIC]

The basic idea for RPC-based TOF-PET

The converter-plate principle

Use the electrode plates as a γ converter, taking advantage of the natural layered construction of the RPCs.

[Blanco 2002]

Stacked RPCs

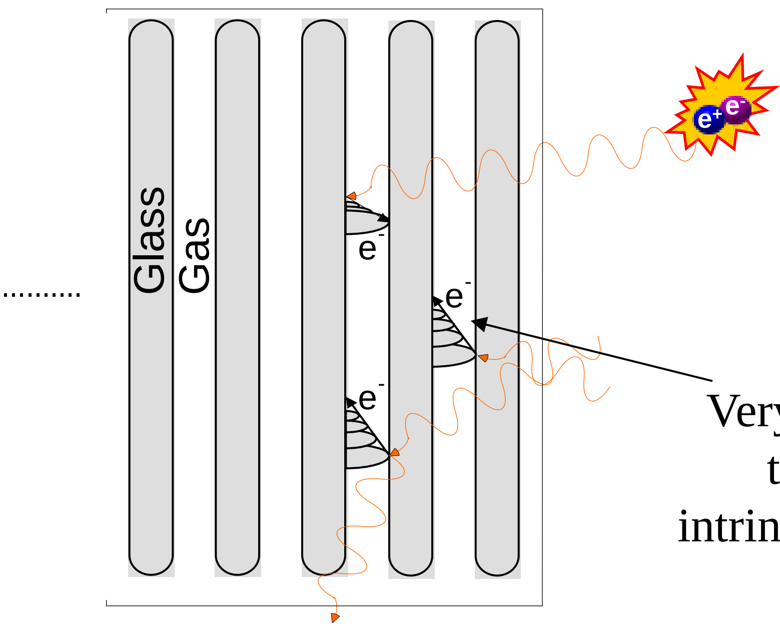

Very small gas gap
to minimize
intrinsic internal error

Time resolution for 511 keV photons:
(our routine lab-test tool)

90 ps σ for 1 photon

300 ps FWHM for the photon pair

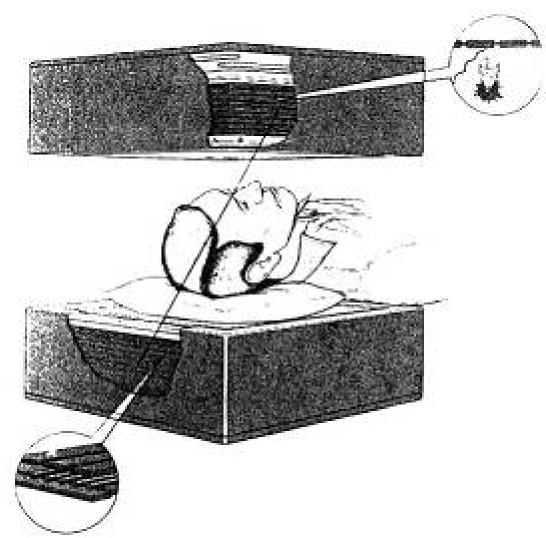

A previous work on PET with gaseous detectors
(21 lead plates + 20 MWPCs = 7% efficiency)

"The Rutherford Appleton Laboratory´s Mark I Multiwire Proportional Counter Positron Camera"
J.E. Bateman et al. NIM 225 (1984) 209-231

Comparison with GEANT - efficiency

Optimum efficiency is balanced by beam absorption (thicker plates) and extraction probability (thinner plates)

Optimum thickness depends on the number of plates and on the material.

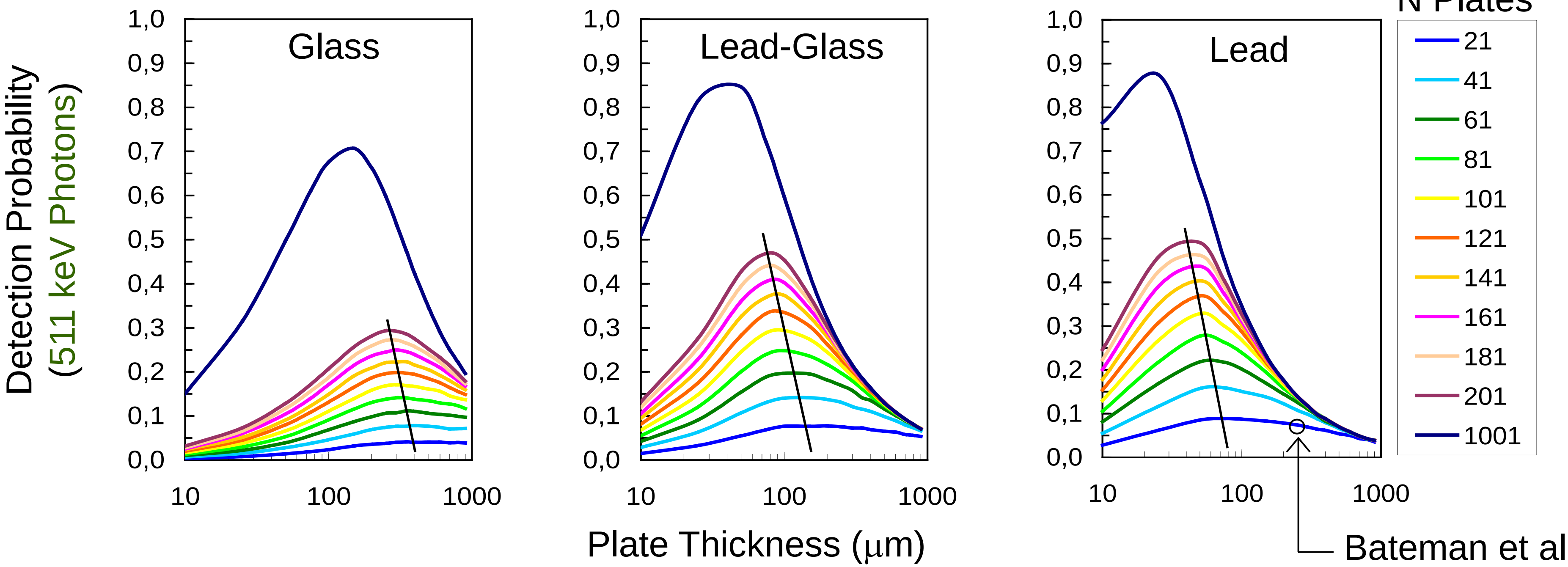

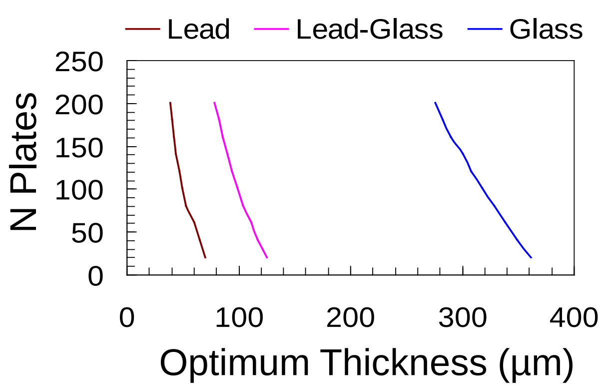

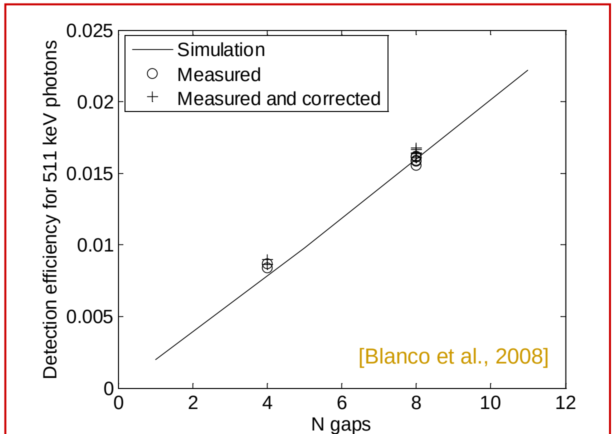

GEANT - energy dependence

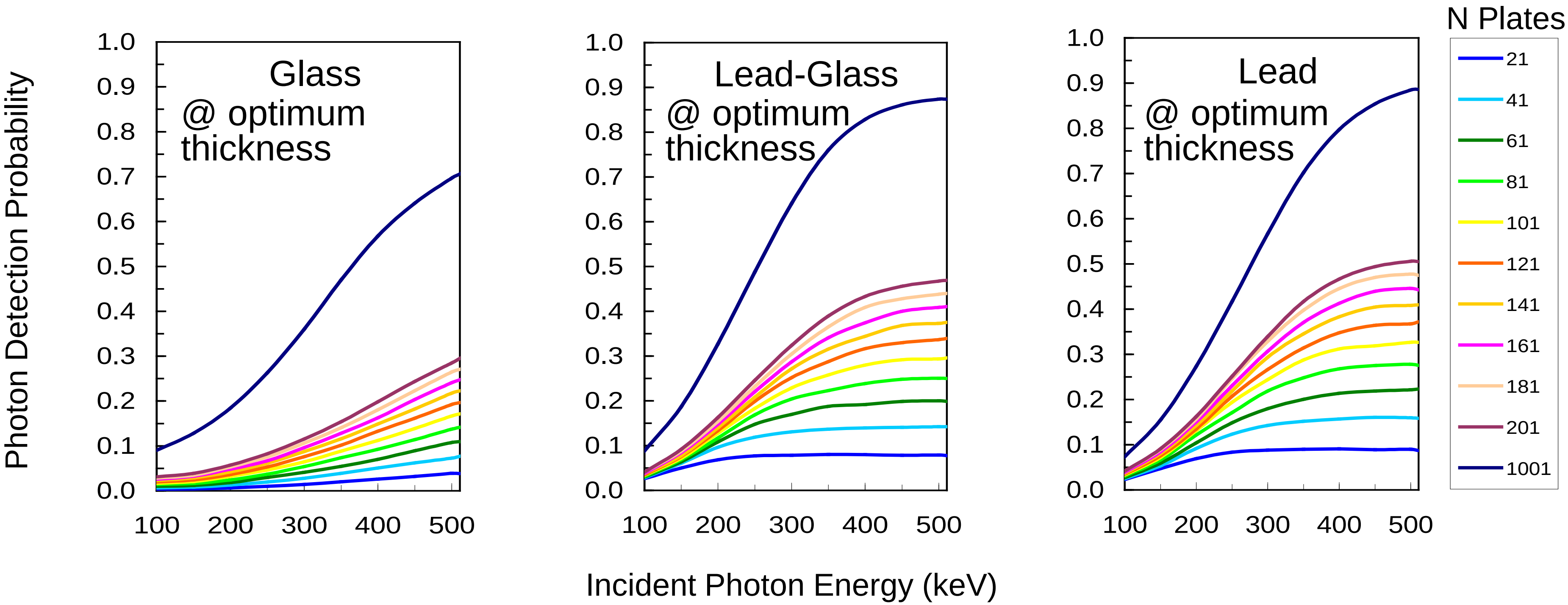

Strong ENERGY SENSITIVY
scattered photons statistically rejected

	ε_{max}	Material: Glass	Lead-Glass	Lead
N Plates	101	*17%*	*29%*	*31%*
	201	*29%*	*47%*	*50%*

Comparison with the standard PET technology

Disadvantages

Certainly a much smaller efficiency: 20 to 50% as compared to 70 to 80%.

No energy resolution, but there is an equivalent energy sensitivity... more later.

Detector scatter (vs. “misidentified fraction” in crystal blocks)

Possible specialized PET applications

Advantages

Increasing system sensitivity

Inexpensive ⇒ large areas possible ⇒ large solid angle coverage

Excelent timing ⇒ TOF-PET possible+optimum randoms rejection

} Whole-body Human PET

Increasing position accuracy

Gaseous detectors routinely deliver 0.1 mm resolution

Full 3D localization possible ⇒ no gross parallax error

The very small gap minimizes intrinsic errors

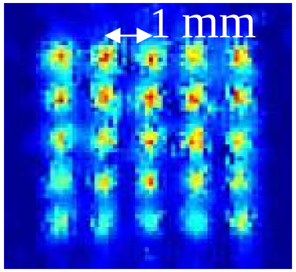

} Small Animal PET

Simulation: 0.51mm FWHM

Other

Simultaneous full body imaging (continuous uptake signal)

Compatible with magnetic field ⇒ PET-MRI can be considered

Small animal PET - a first prototype

Aimed at **verifying** the concept and show the **viability** of a **sub-millimetric spatial resolution**.

Charge-sensitive electronics allowing interstrip position interpolation

16 stacked RPCs

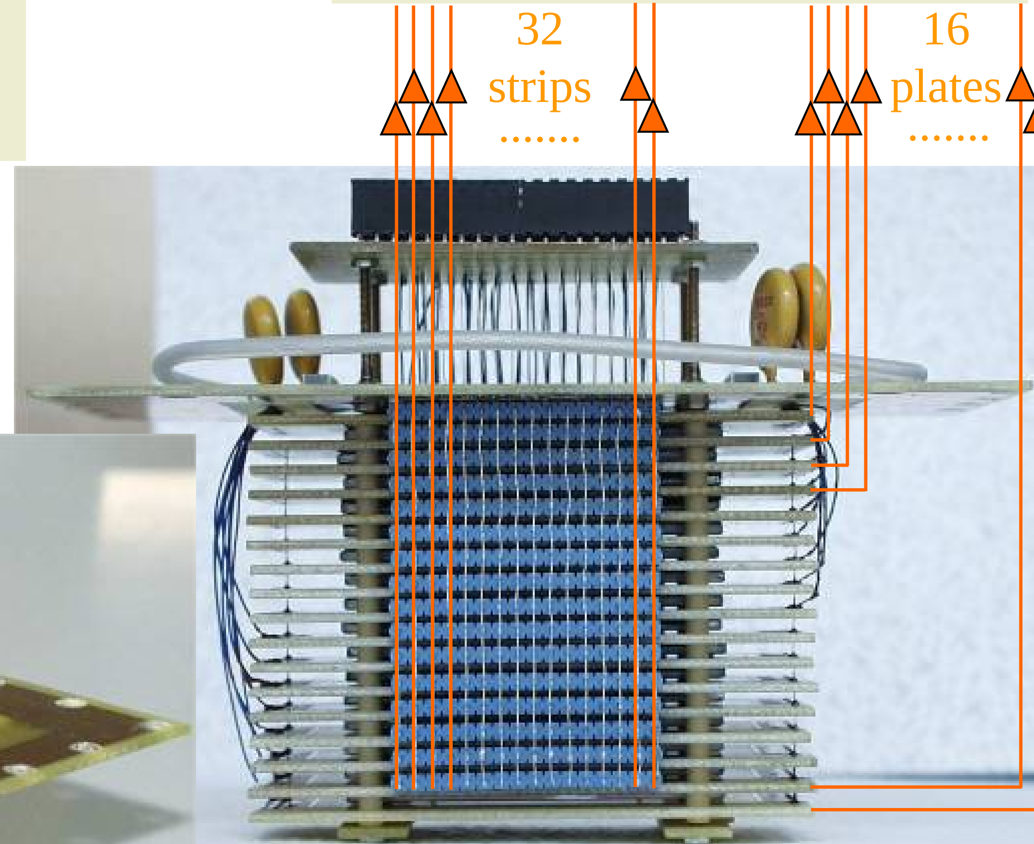

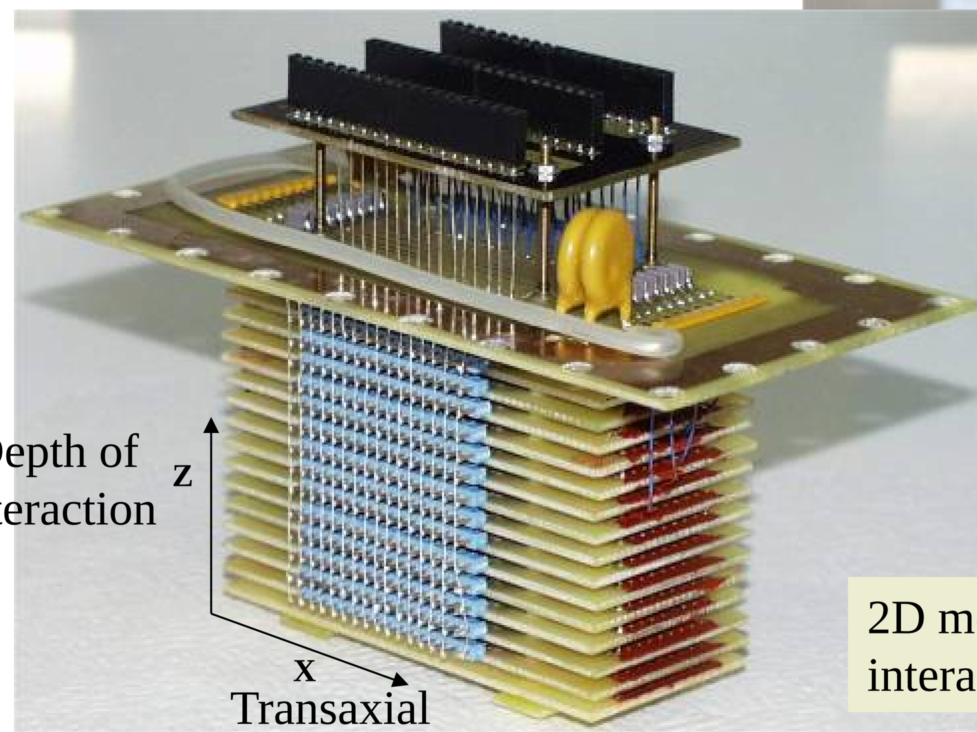

2D measurement of the photon interaction point

System

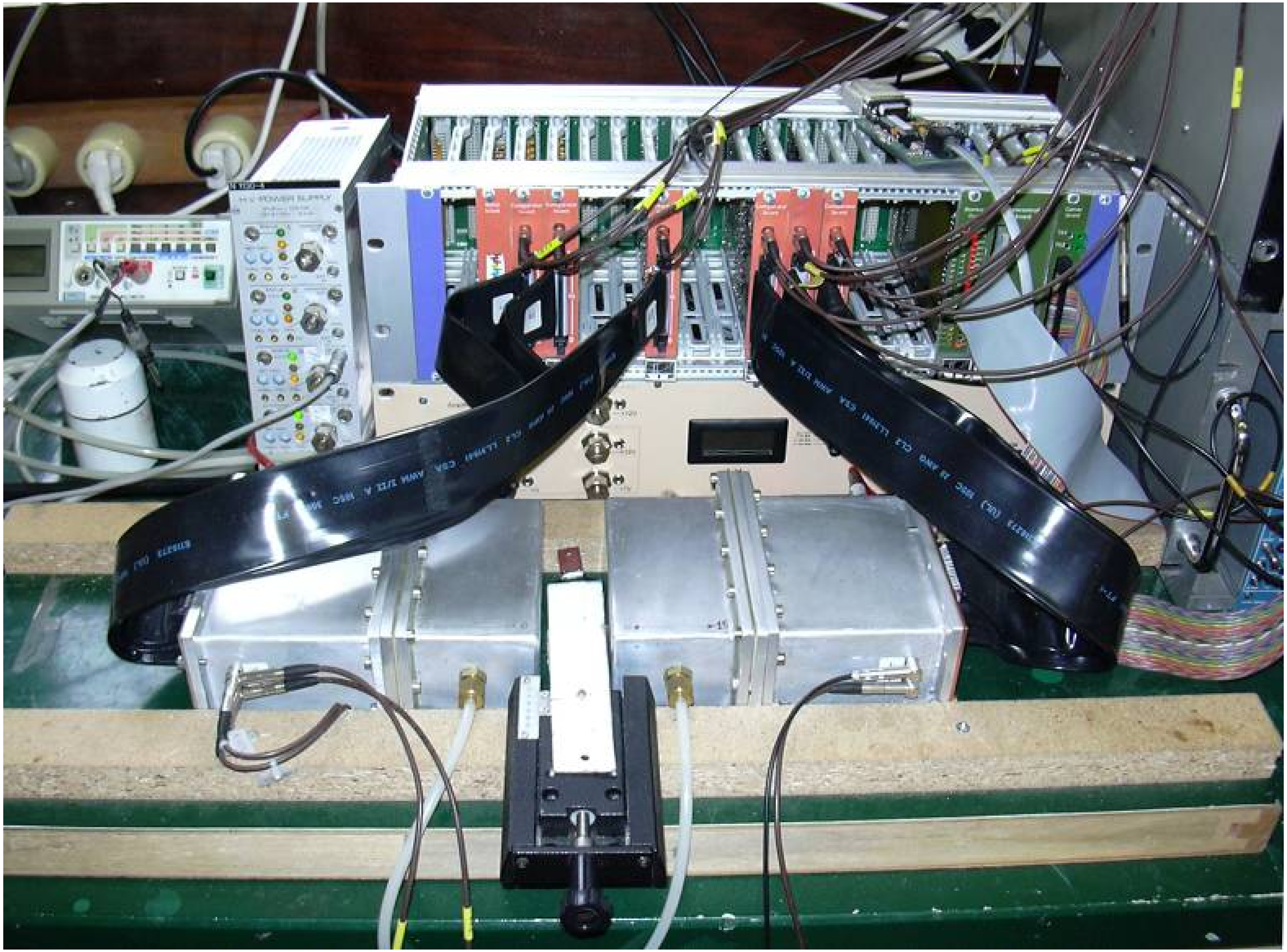

Intrinsic spatial resolution

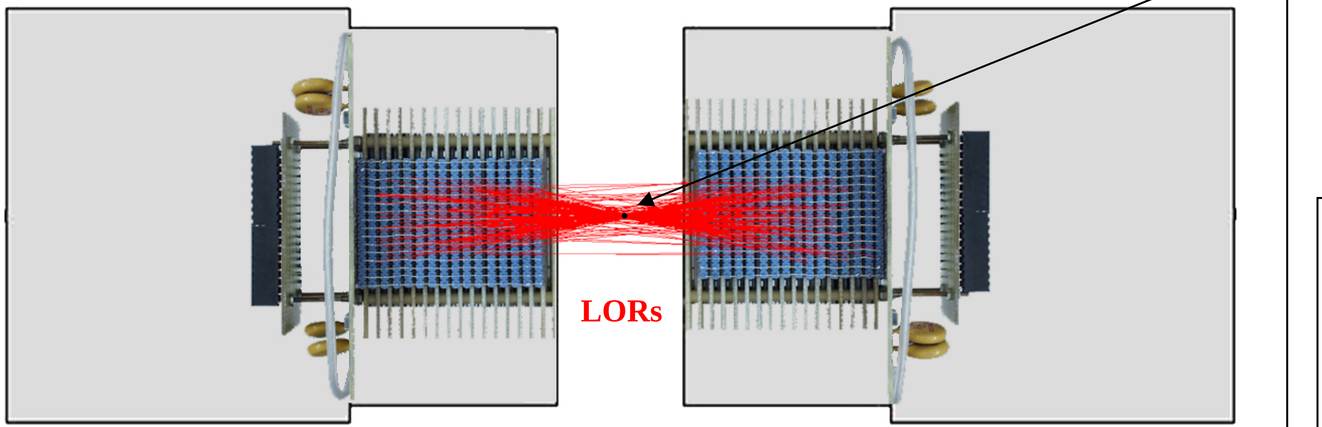

Red lines correspond to real data acquired with the ^{22}Na source

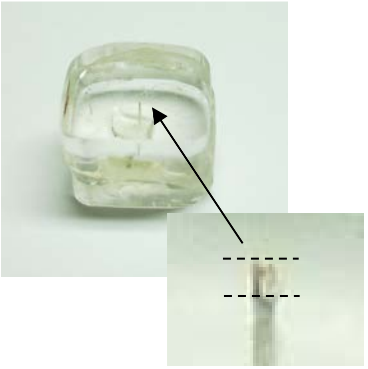

Custom-made ^{22}Na source

0.22 Ø x 0.5 mm

LOR = Line of Response. Connects the interaction points of the photons.

D = Distance between each LOR and the center of the system

Image spatial resolution (gaussian fitting)

Filtered Back Projection FBP

~ 465 µm FWHM

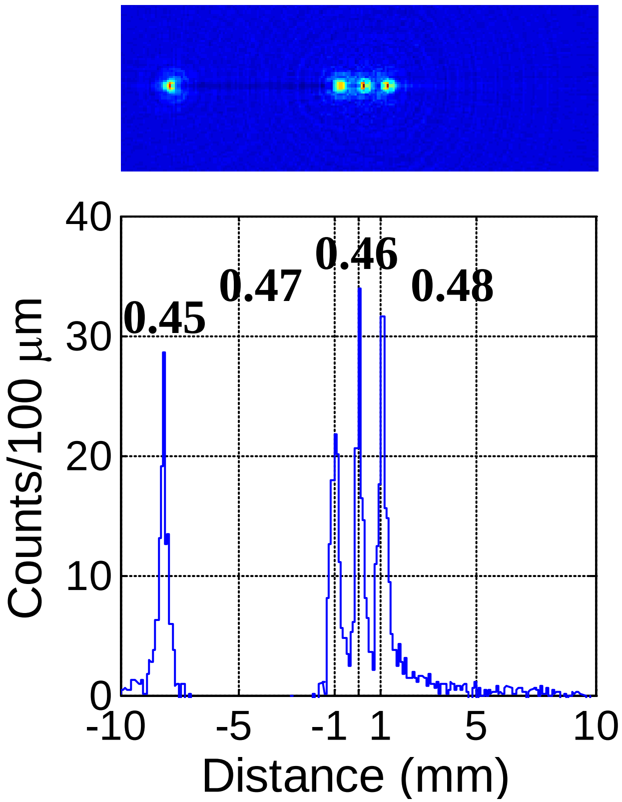

Maximum likelihood-expectation maximization with resolution modeling (ML-EM)

~ 305 µm FWHM

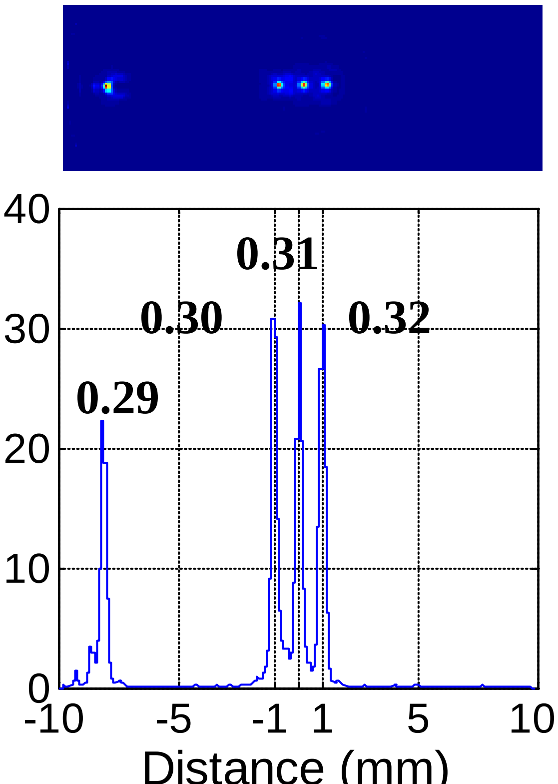

Proceeding IEEE MIC (2004) M2-177

[Blanco, IEEE MIC 2004]

Homogeneous spatial resolution over the entire detector

Simulated count rate performance

Evaluation of the count rate performance Prompts, Randoms, and NECR

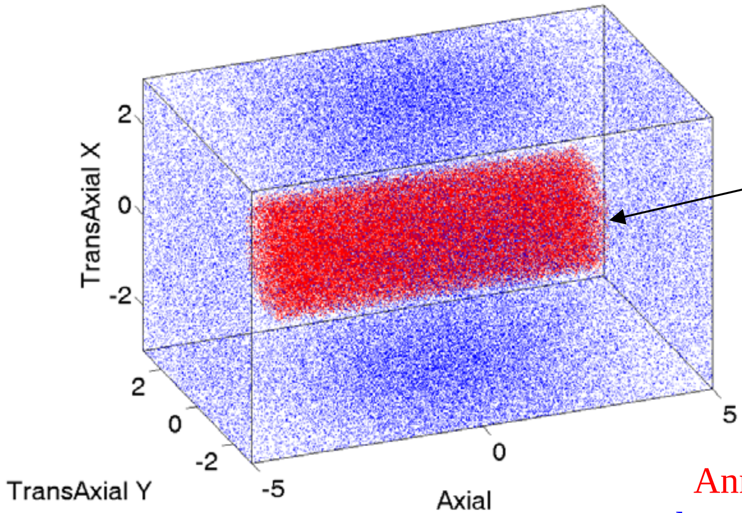

Mouse size phantom:

25 Ø x 70 mm (34 cm^3)

Annihilations and photons on the detector surface from the simulation.

GEANT4

Characteristic of the simulated system:

- **90% Solid angle coverage** => defining a FOV of 60 Ø x 100 mm axial.
- Narrow **coincidence window 1 ns. (Timing resolution 300 ps FWHM)**
- **Dead time ~ 100 ns.**
- **10% - 15% detection efficiency.**

[Blanco, IEEE MIC 2004]

Performance – small animal PET

Comparison between different small animal PET parameters and the expected parameters of the RPC-PET.

Scanner	Image spatial Resolution, FBP (mm)	Time resolution (ns FWHM)	FOV (mm Ø x mm)	Central point absolute sensitivity (cps/kBq)	Source (mm Ø x mm)	Peak NEC (Kcps)
microPET II® [1],[2]	1.1	3	160 x 49	23 - 33	25 x 70 mouse size	235 at ~2.35 MBq/cm^3
microPET Focus F120 [6]	1.75	6	147 x 76	71	mouse size	809 at ~88 MBq
YAP-PET [3],[4]	1.6	2	40 x 40	18 at (Ø = 150 mm)	-	90 (not peak) at ~16.6 MBq
Quad HIDAC (32 modules) [5]	0.95	-	170 x 280	18	-	100 at ~0.2MBq/cm^3
RPC-PET	0.51	0.3	60 x 100	21	25 x 70 mouse size	318 at ~ 2.63 MBq/cm^3 (simulated)

1. Yuan-Chuan Tai et al., "MicroPET II: design, development and initial performance of an improved MicroPET scanner for small-animal imaging", *Phys. Med. Biol.* 48 (2003) 1519-1537.
2. Yongfeng Yang, et al., "Optimization and performance evaluation of the microPET II scanner for in vivo small-animal imaging", Phys. Med. Biol. 49 (2004) 2527-2545.
3. A. del Guerra, G. Di Domenico, M. Scandola, G. Zavattini, "YAP-PET: first results of a small animal Positron Emission Tomograph based on YAP:Ce finger crystals", IEEE Trans. Nucl. Sci., vol 45, No. 6 December 1998, 3105-3108.
4. G. Di Domenico et al., "Characterization of the Ferrera animal PET scanner", Nucl. Instr. And Meth. A, 477 (2002) 505-508.
5. A.P. Jeavons, R.A. Chandler, C.A.R. Dettmar, "A 3D HIDAC-PET Camera with Sub-millimetre Resolution for Imaging Small Animals", IEEE Trans. Nucl. Sci., vol. 46, No. 3, June 1999, 468-473.
6. Richard Laforest et al. "Performance Evaluation of the microPET – Focus F120", presented at IEEE NSS/MIC Rome 2005.

[Blanco, IEEE MIC 2004]

Full scanner for mice in construction

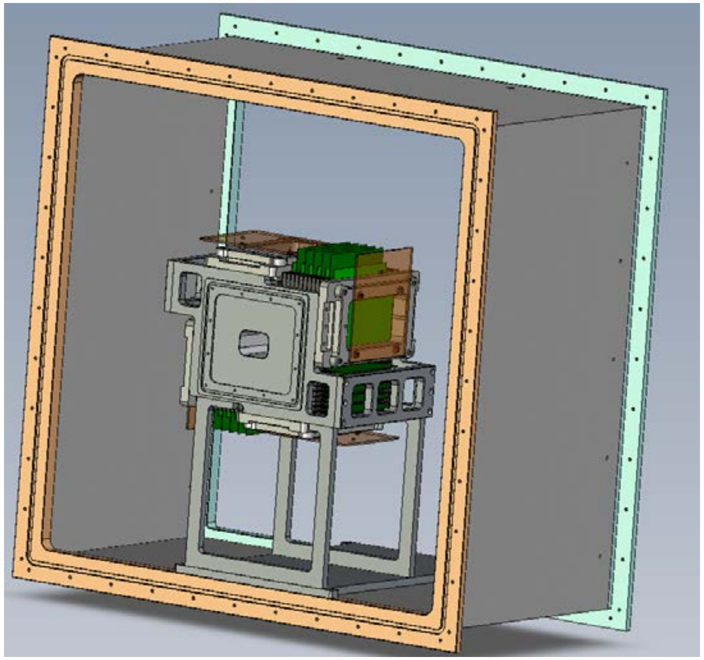

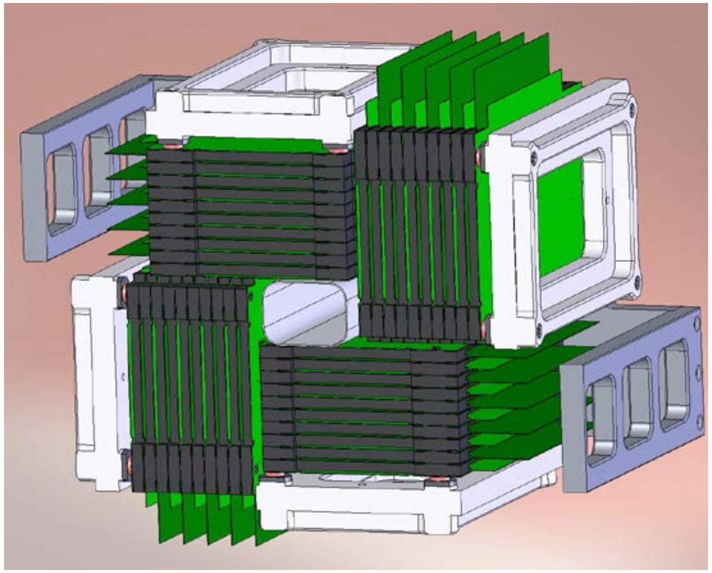

Expected quantum efficiency and resolution with FBP

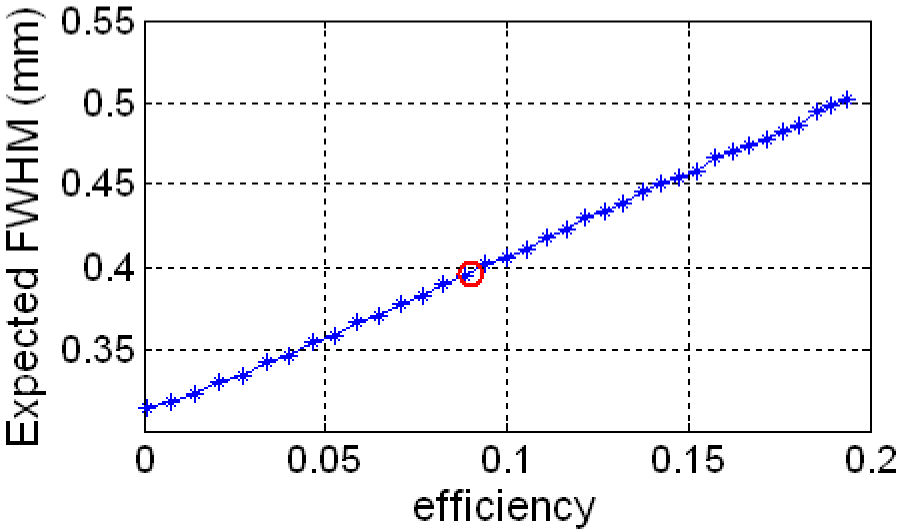

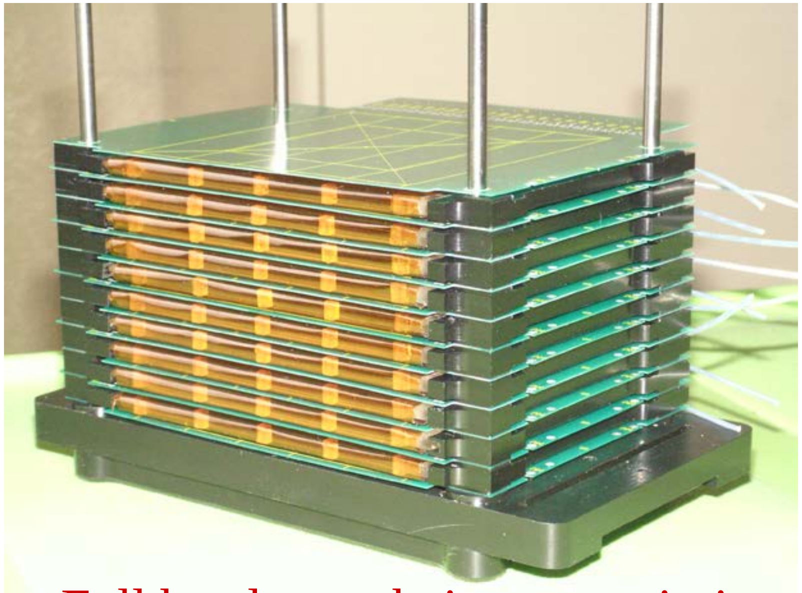

Full head, now being commissioned

Resolution tests

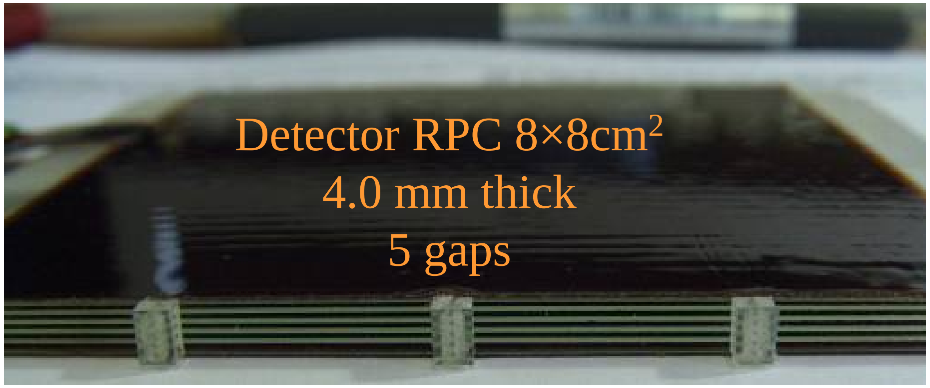

Needle source, 0.2 mm ⌀ int.

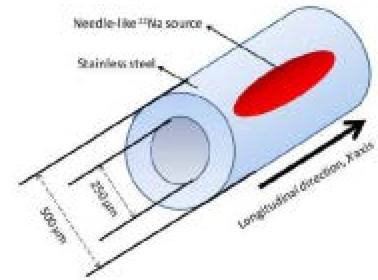

Two detectors with XY localization

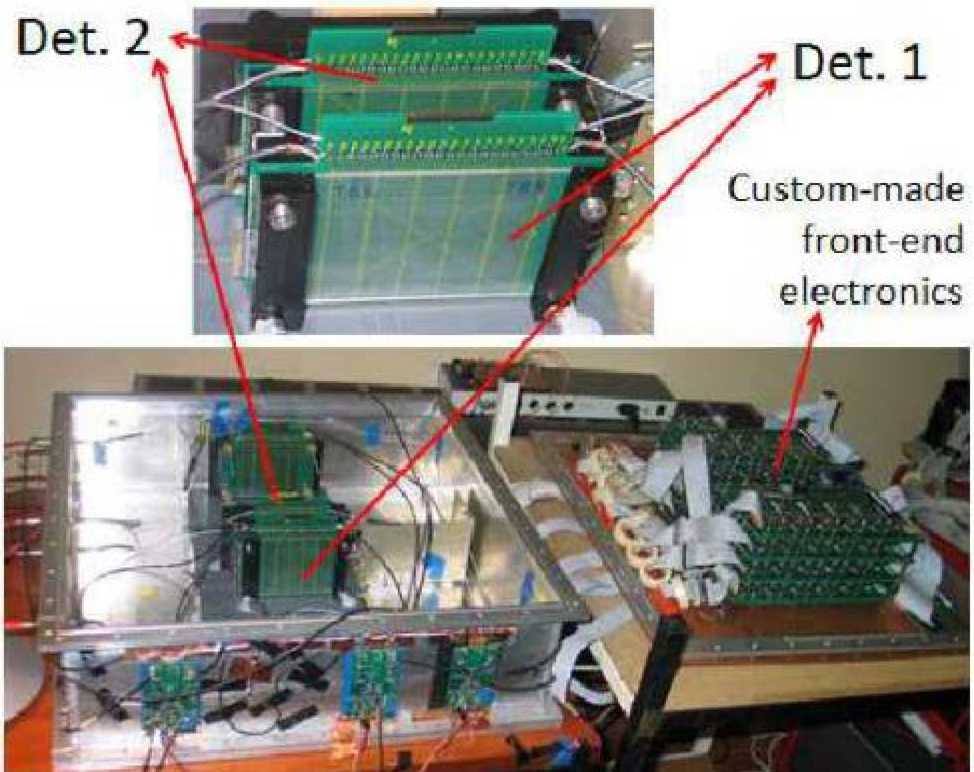

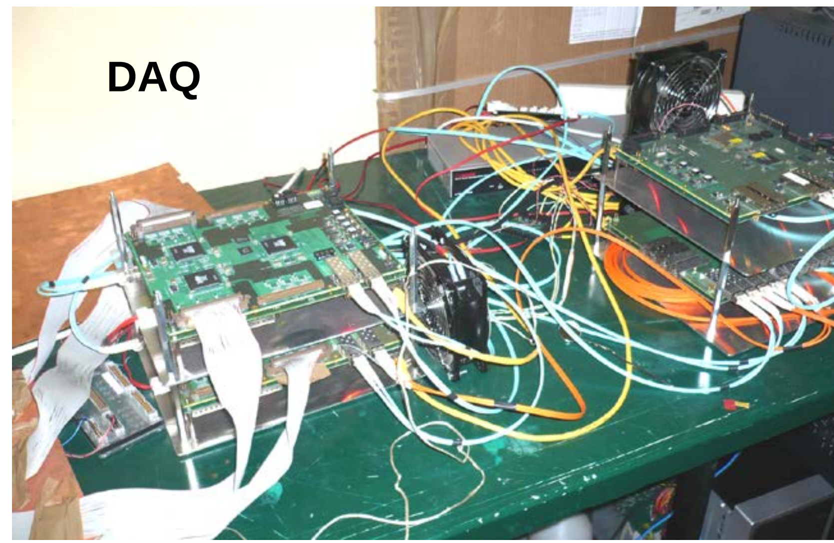

Provided by the HADES DAQ group GSI, IKF (Germany) and JU (Poland).

Resolution tests (needle source)

Full area, all angles, all gaps
MLEM reconstruction

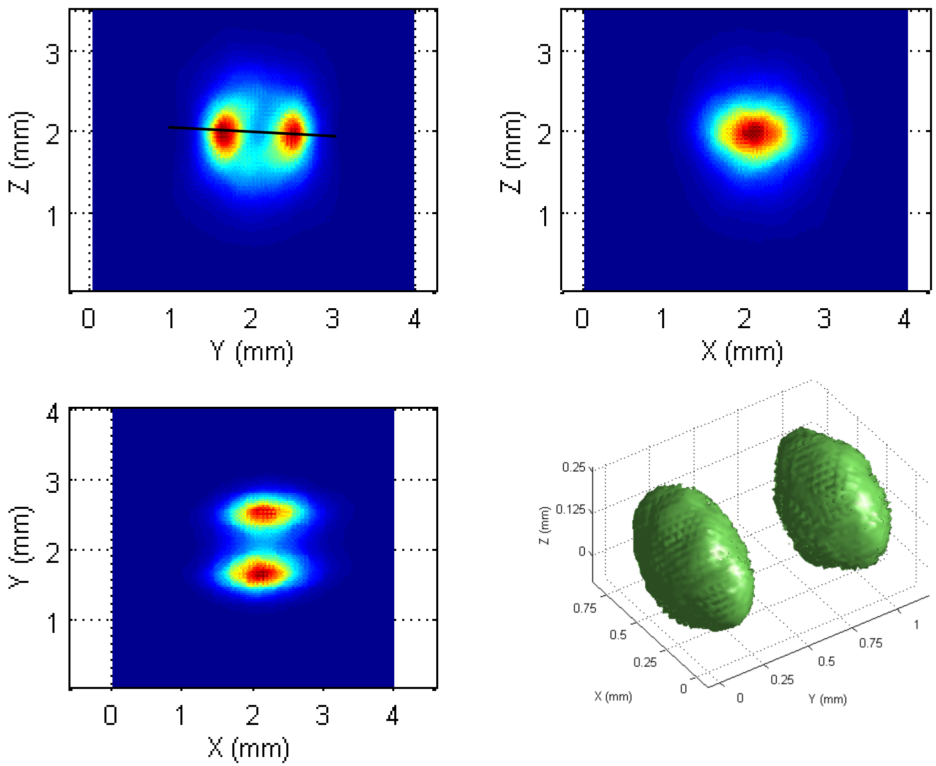

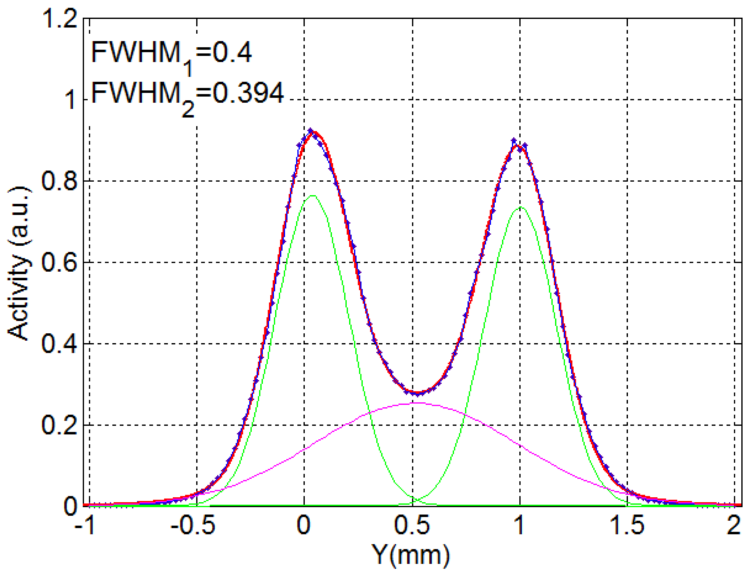

Joint reconstruction of the source in 2 positions separated by 1mm.
Color maps: planar profiles including peak density point.
Isosufaces: 50% rel. activity

Reconstructed activity profile across the black line shown in the upper left panel.
Resolution ~0.4mm FWHM
+background
(Note: source is 0.2mm diam.)

Resolution tests (disk)

older data in non-optimized conditions

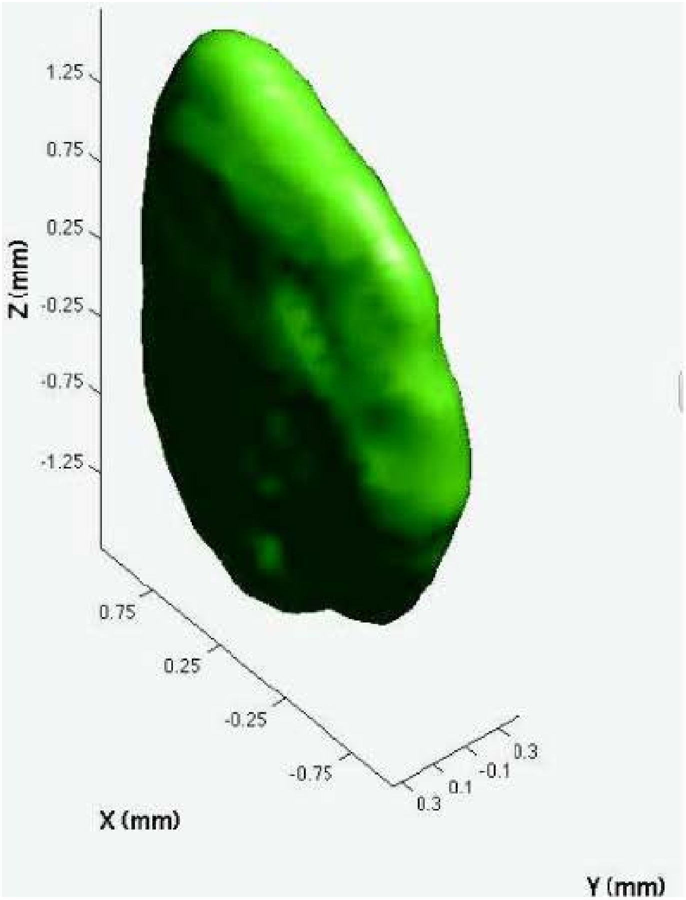

50% isoactivity surface

^{22}Na disk source edge-on (0.2mm bins)

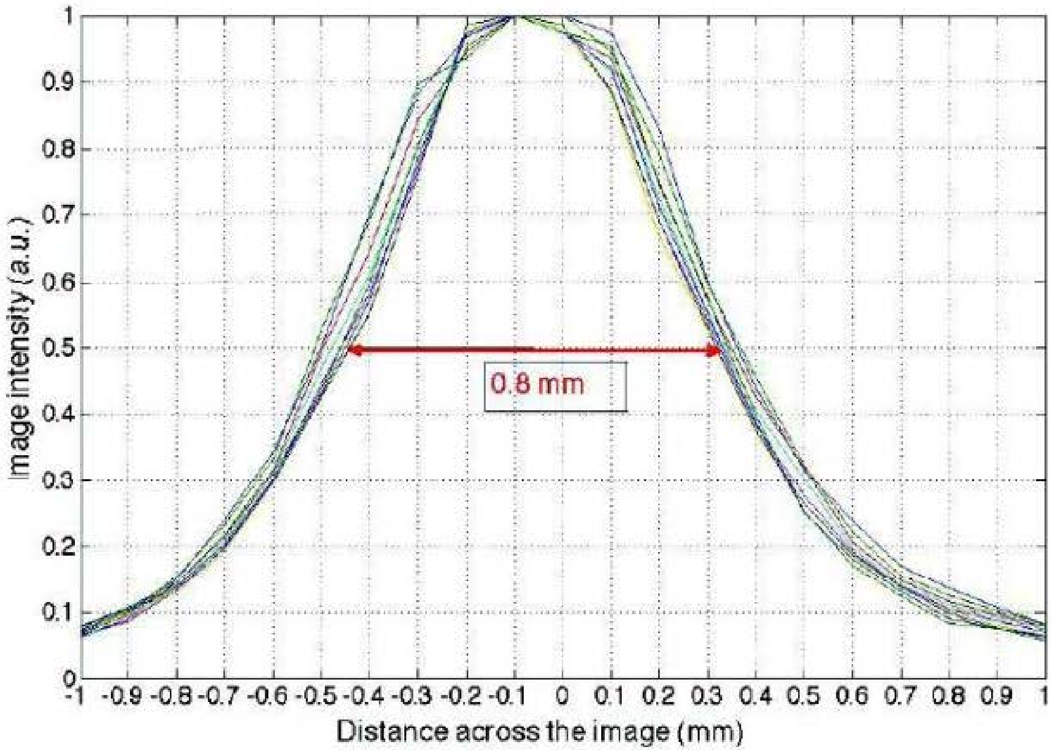

Profiles across image (0.8mm FWHM)

Full-body human RPC TOF-PET

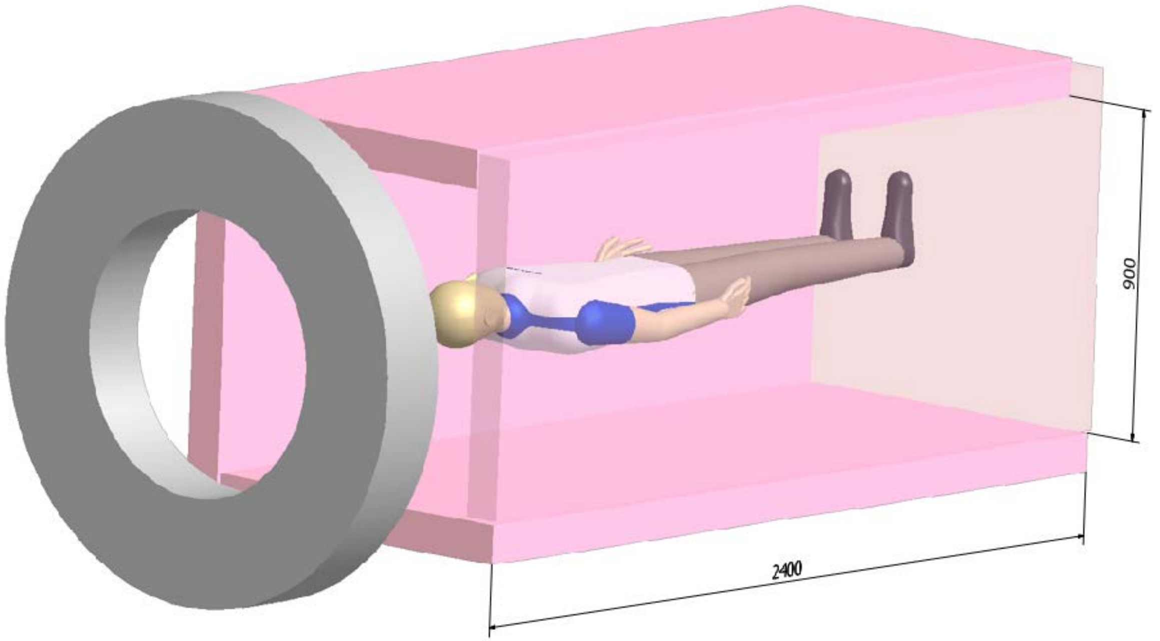

The importance of high sensitivity in PET

$$\text{Image quality} \propto \text{counts/pixel}$$

$$\text{counts/pixel} \propto \frac{\text{activity injected in patient} \times \text{measurement time}}{\text{number of pixels}} \times \text{sensitivity}$$

Lower the injected dose
⇒ PET exam can be used on lower risk patients

Higher resolution possible
⇒ Smaller tumours visible

More examinations per unit time
⇒ Lower examination costs
⇒ More people can afford PET exams

Lives saved through earlier cancer detection?

RPC TOF-PET – sensitivity advantage

Simulations performed in GEANT 9.1.p01

Applied the RPC energy-sensitivity curve on an otherwise ideal detector (no scatter in detector)

Efficiencies of 60 and 120 stacked RPCs
based on 0.4 mm glass plates

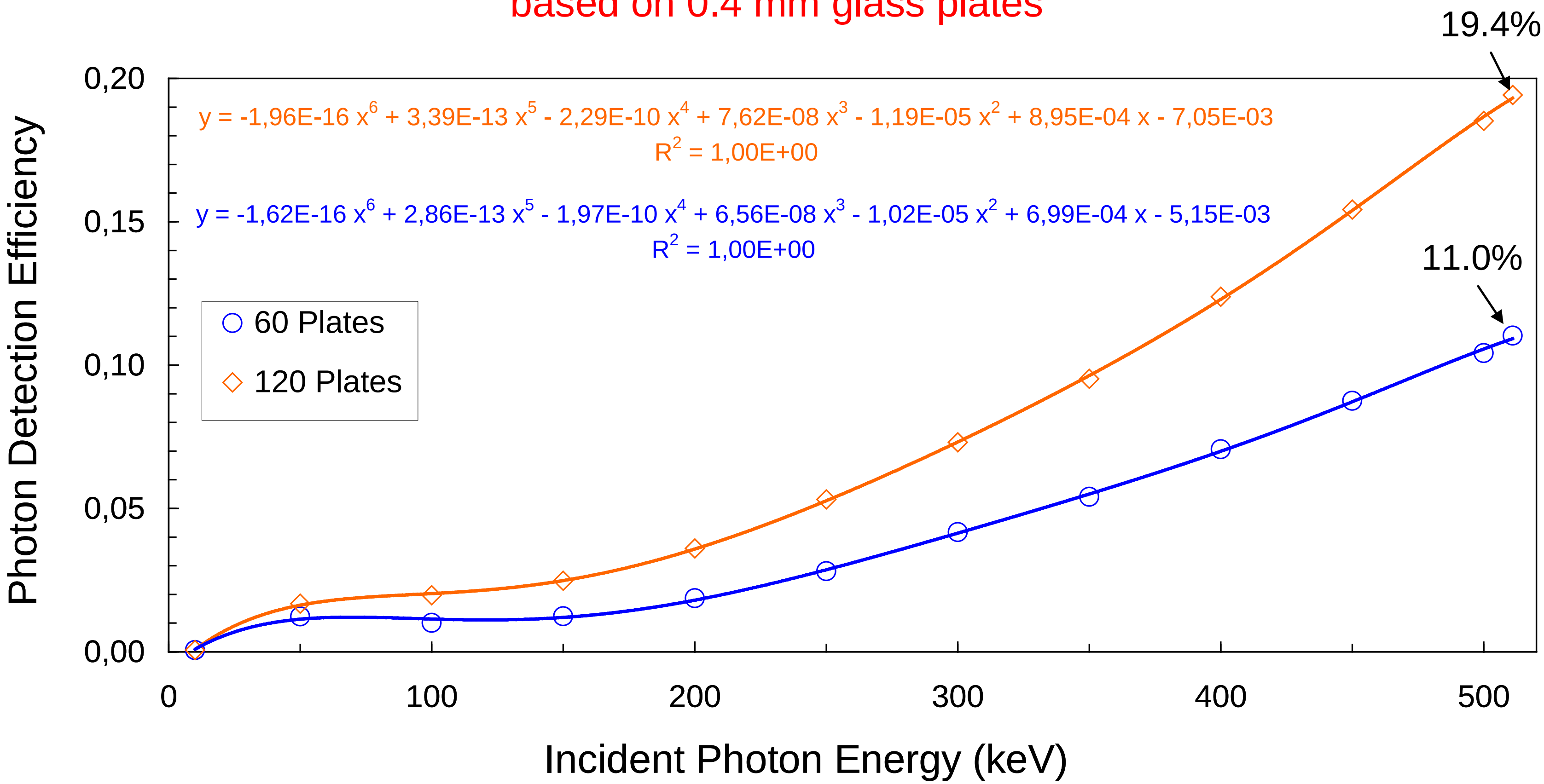

[P.Crespo et al., 2009 IEEE MIC]

RPC TOF-PET – sensitivity advantage

Table 2: Sensitivity performance of several PET scanners simulated with Geant4.

	PET scanner	Biograph[a] TruePoint	Biograph[a] TruePoint TrueV	GE[b] Advance (3D-mode)	196-cm AFOV LSO-based	RPC-PET
	Nb. of block-rings	3[c]	4[c]	3[d]	35[c]	n.a.
	AFOV (cm)	16.2	22	15.2	196	240
	Ring difference	27	38	11	162	$\theta \leq 45°$ [e]
	Packing fraction	0.86	0.86	0.844	0.86	1.0
	Crystal depth (cm)	2.0	2.0	3.0	0.43	n.a.
	Singles efficiency at 511 keV	0.7	0.7	0.78[f]	0.194	0.194
LS in water phantom[n]	Absolute sensitivity, η_a 1.5-m line source (%)	0.013	0.023	0.019	0.066	0.172
	Planar sensitivity[k], η_s (% per 2-mm slice thickness)	0.239	0.327	0.342	0.079	0.158
	Time for equal image quality[l] (min:sec)	2:04 [5]	1:30 [5]	1:27	6:15	3:08
	Scan of 1.5-m length object					
	Nb. of bed steps	14	11	14	1	1
	Total scan time (min:sec)	28:56	16:30	20:18	6:15	3:08
	Relative gain (no TOF)[m]	**1.0**	**1.8**	**1.4**	**4.6**	**9.2**
	Relative gain (with TOF)[m]	**3.0**[o]	**5.4**[o]	n.a.	**13.8**[o]	**55.2**[p]

[P.Crespo et al., 2009 IEEE MIC]

~30-fold sensitivity increase over current state-of-the art scanners

~10-fold if TOF (600 ps) is introduced to LSO scanners

The real benefit of the TOF information is a matter of current research

In here we used the formula:

$$\text{TOF sensitivity advantage} \approx \frac{\text{object size}}{(c/2)\ \text{time resolution}}$$

1) NECR – Noise Equivalent Count Rate

a) Simulation Setup

- Simulations performed with GEANT4, release 9.2, patch 4
- Scanner with parallelepipedic shape, with 4 detection walls, each of them containing 20 RPC detectors (~2400x1000x6.8 mm), with 10 gaps (350 μm thick) and glass resistive electrodes (200 μm thick)
- NEMA NU2–2001 Scatter Fraction Phantom centered in the Field Of View
- Source consists on the decay of ^{18}F at rest, uniformly distributed in the phantom line source, with photon non-collinearity provided by GATE

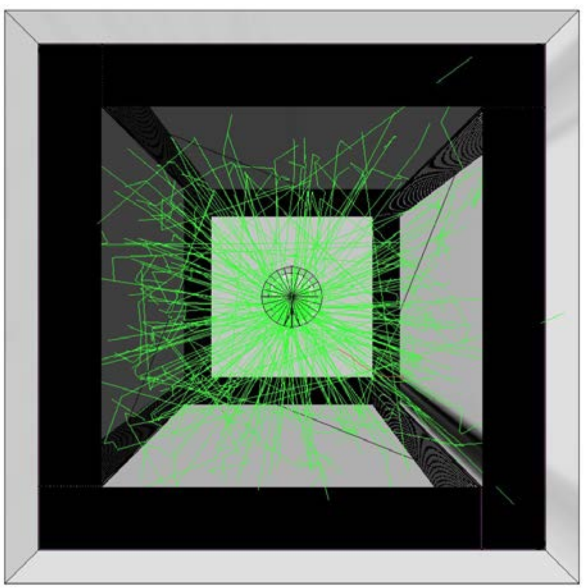

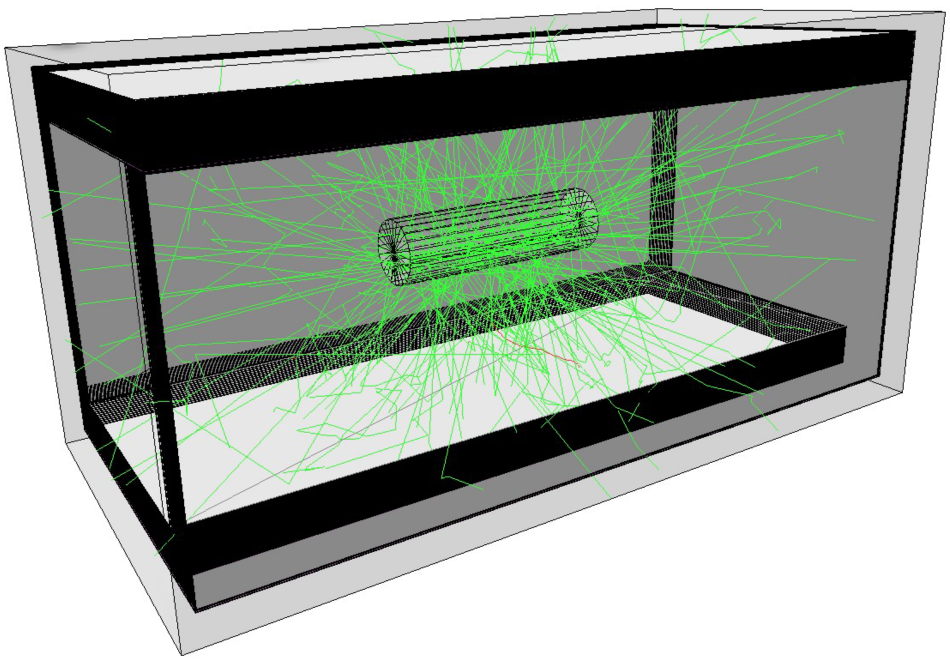

[M.Couceiro PhD thesys]

Calculations performed at the MILIPEIA cluster of Laboratório de Computação Avançada of U.C.

1) NECR – Noise Equivalent Count Rate

c) Phantom Geometry

- Solid right circular cylinder
  - Material: polyethylene with 0.96 specific gravity
  - Dimensions: 20 cm outside diameter and 70 cm overall length
  - Source: right circular cylinder with 3.2 mm inside diameter and 70 cm length, filled with ^{18}F diluted in water

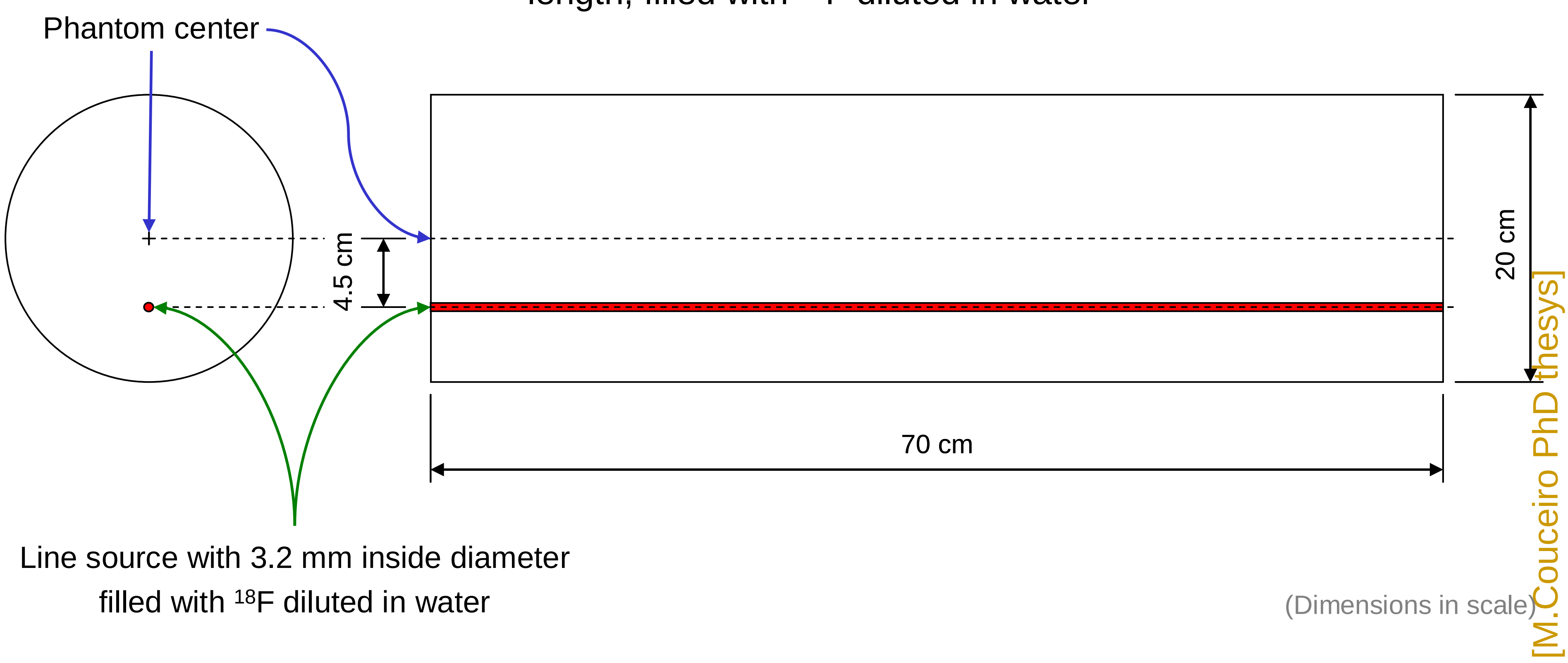

Readout strategy

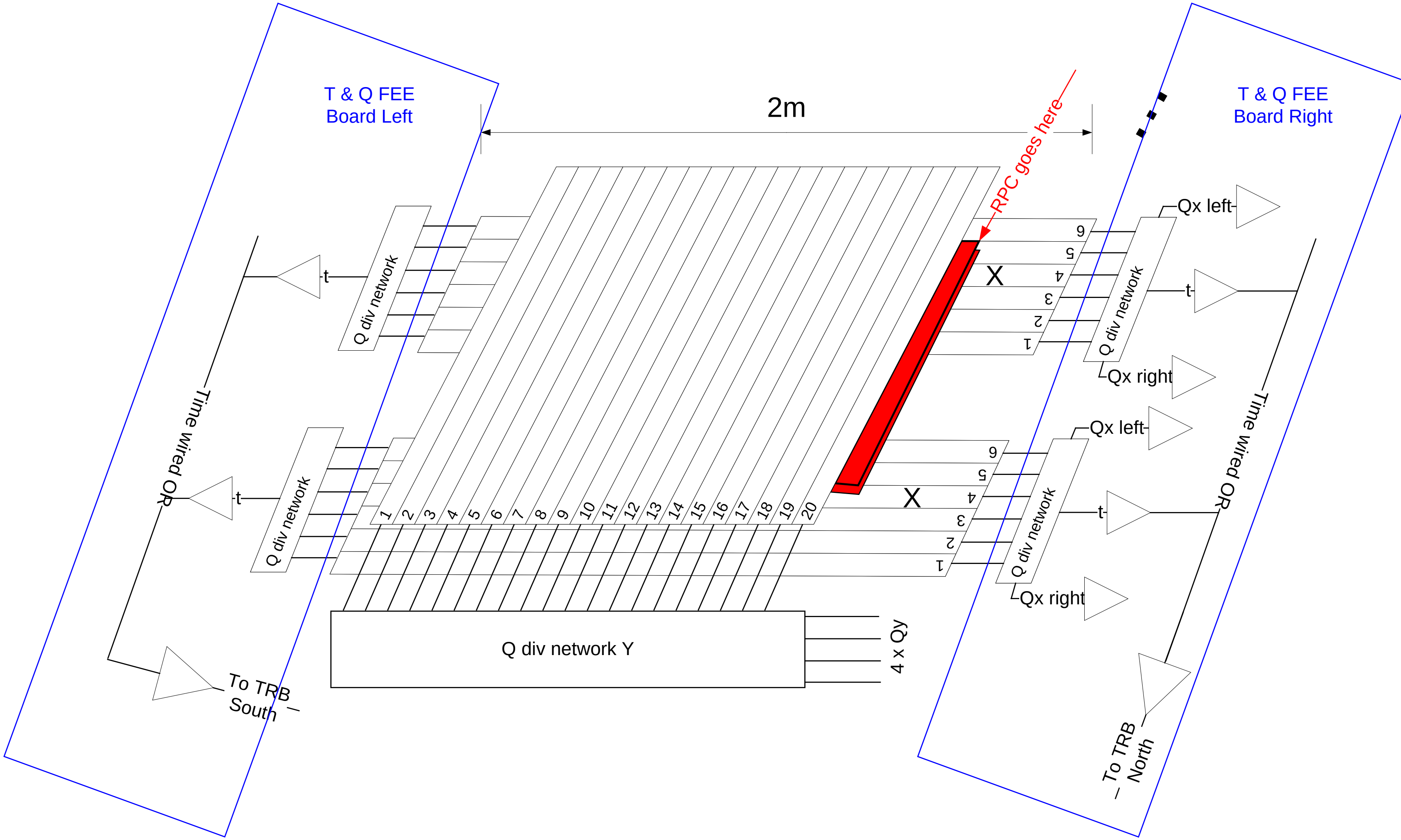

Scanner is composed by 800 independent readout “sections”, each measuring XY position and time for a single hit.

[Patent pending]

1) NECR – Noise Equivalent Count Rate

e) Multiple Hits Rejection

- After readout processing, multiple photon hits are removed by time-space considerations

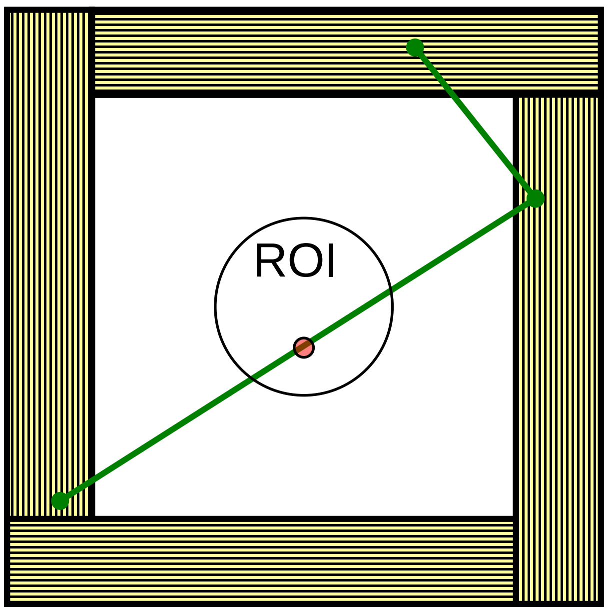

Scatter Fraction profiles for the axially extended phantom.

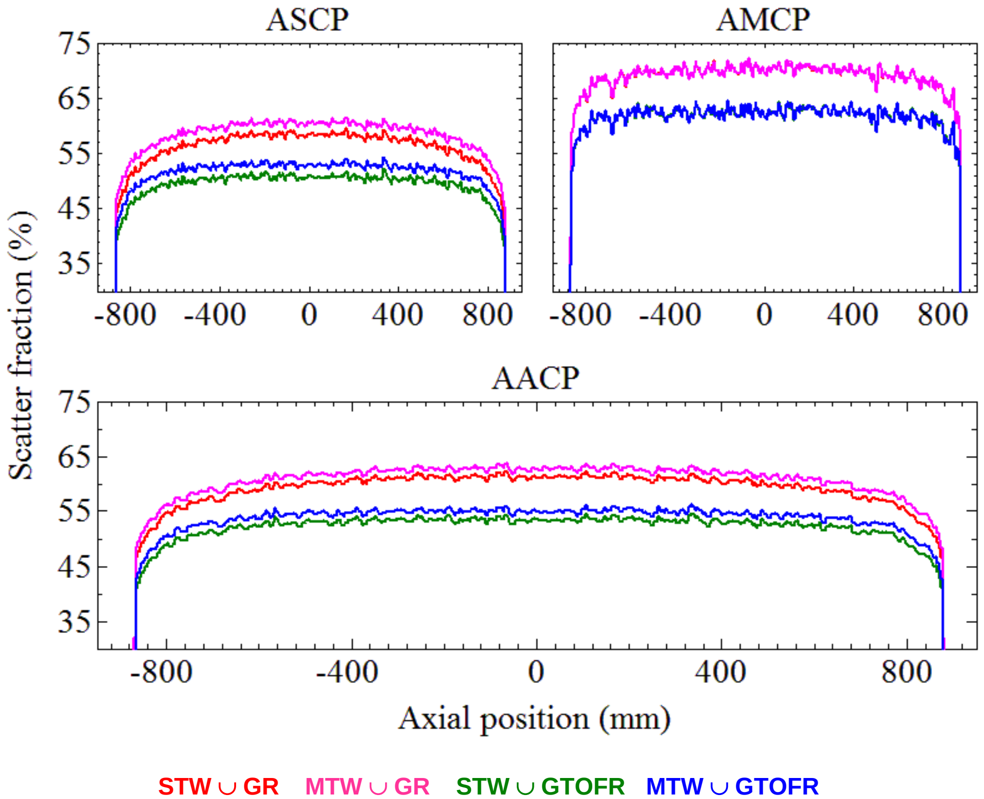

[M.Couceiro PhD thesys; P.Martins et al.,2012 IEEE NSS/MiC]

1) NECR – Noise Equivalent Count Rate

[M.Couceiro PhD thesys]

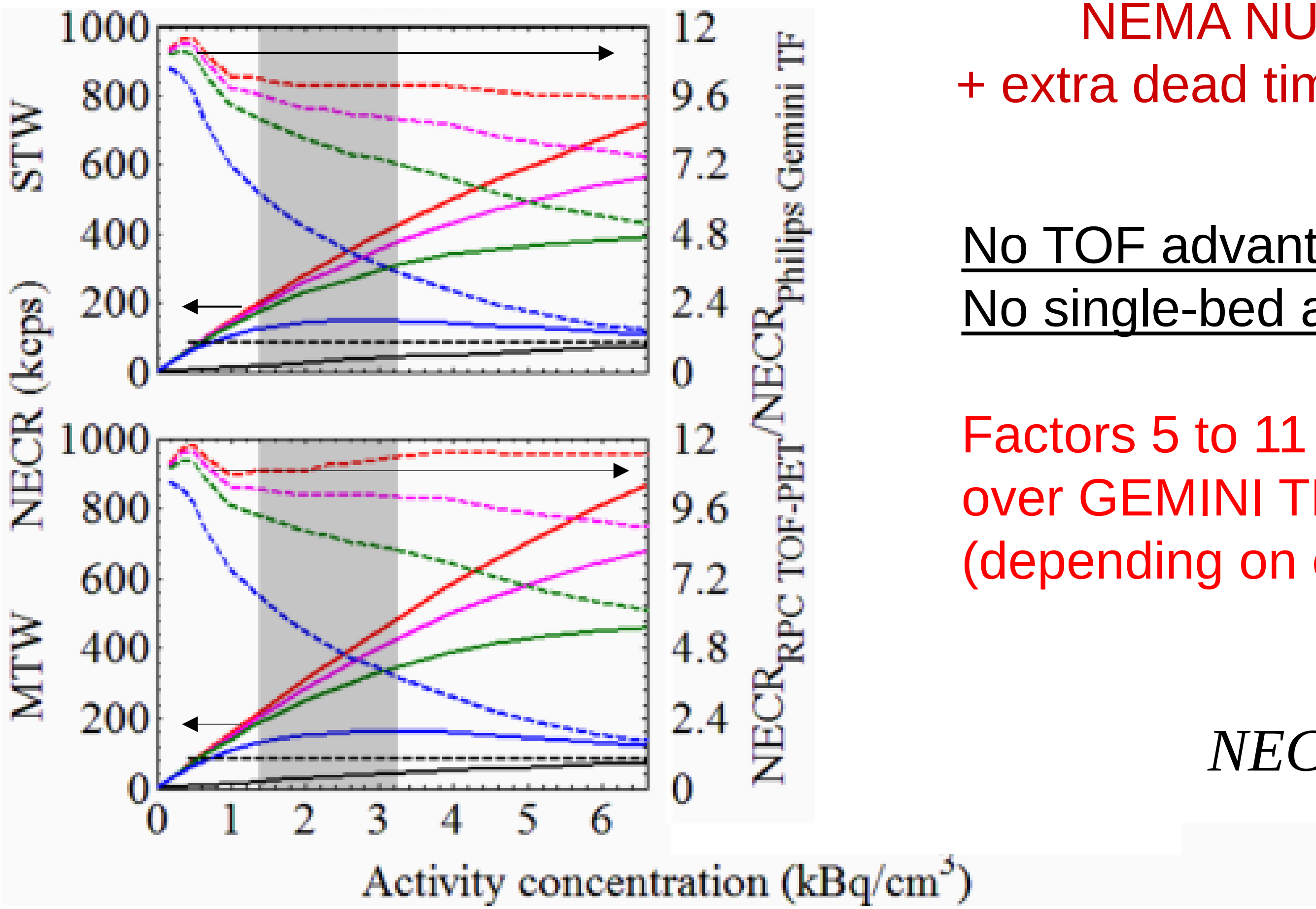

NEMA NU2-2001 - like
+ extra dead time for fine position

No TOF advantage considered
No single-bed advantage

Factors 5 to 11 NECR advantage over GEMINI TF
(depending on electronics dead time)

$$NEC = \frac{T^2}{T + S + 2R}$$

$\tau_{ps} = 0.0\ \mu s$ $\tau_{ps} = 0.5\ \mu s$ $\tau_{ps} = 1.0\ \mu s$ $\tau_{ps} = 3.0\ \mu s$

$NECR \rightarrow$ left Y axes

$\frac{NECR_{RPC\ TOF-PET}}{NECR_{Phylips\ Gemini\ TF}} \rightarrow$ right Y axes

Prototype detecting head (30×30cm^2 × 8 gaps)

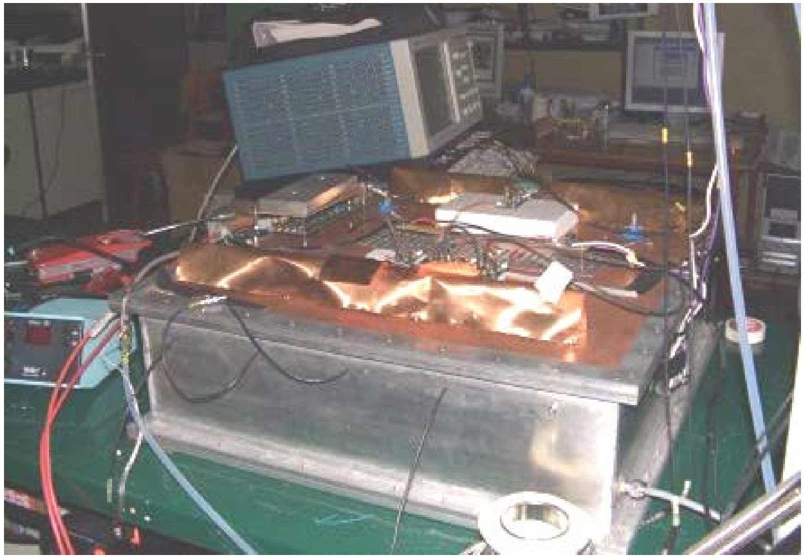

Time resolution – 300 ps FWHM

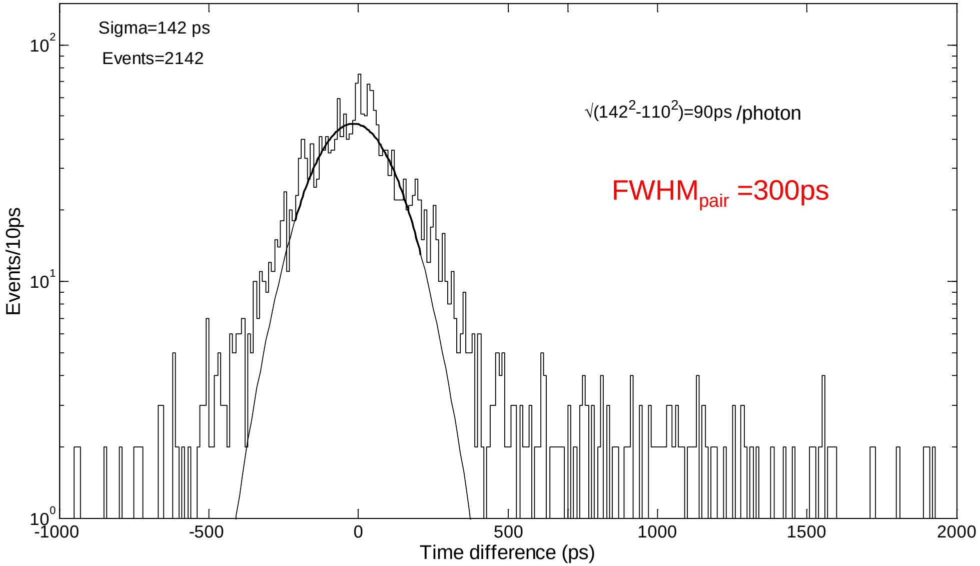

Efficiency as expected from GEANT

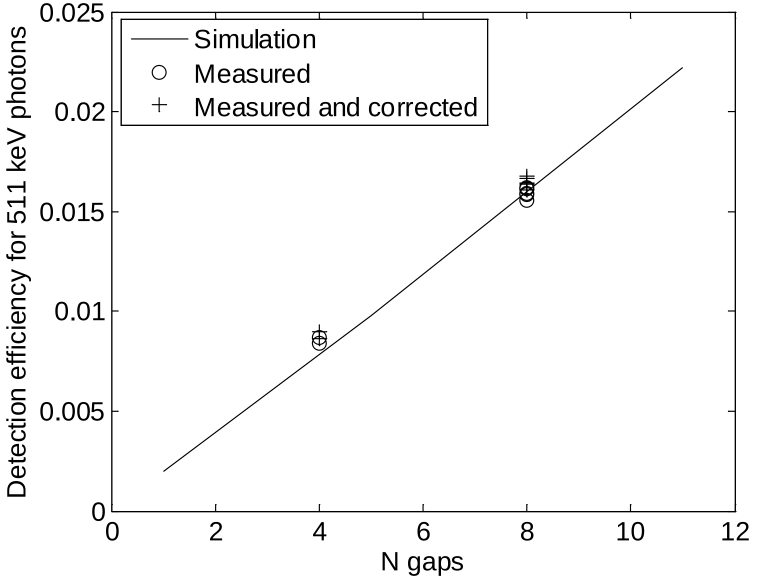

Prototype of human RPC-PET in development

Prototype of the basic human RPC-PET detector module

Characteristics:

- 6 glasses of 150±10 µm (a bit too thin)
- 5 gas gaps of 350 µm
- active area 870x415 mm (x6=~2.4m long)
- all high voltage and gas distribution inside

Readout tests

Many subsystems already tested

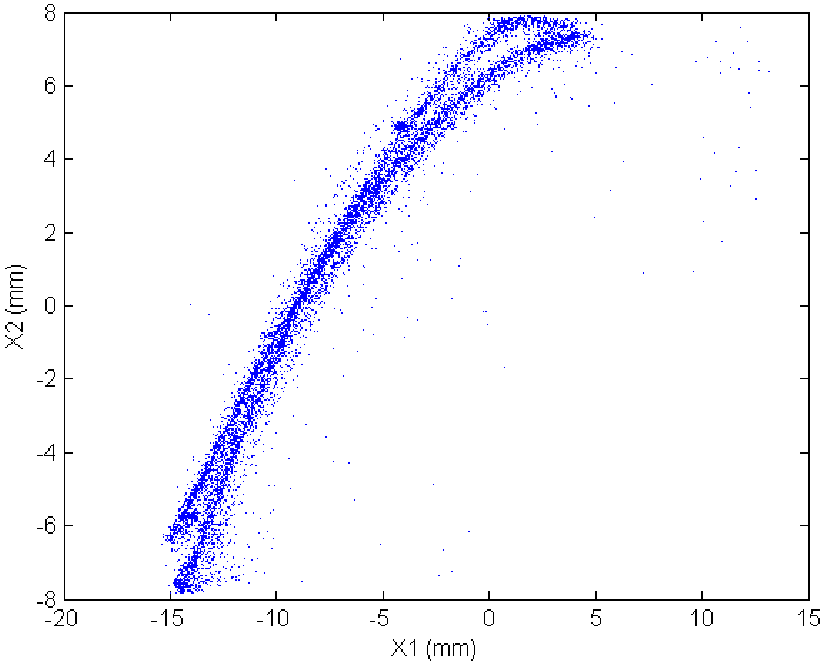

Xup vs. Xdown

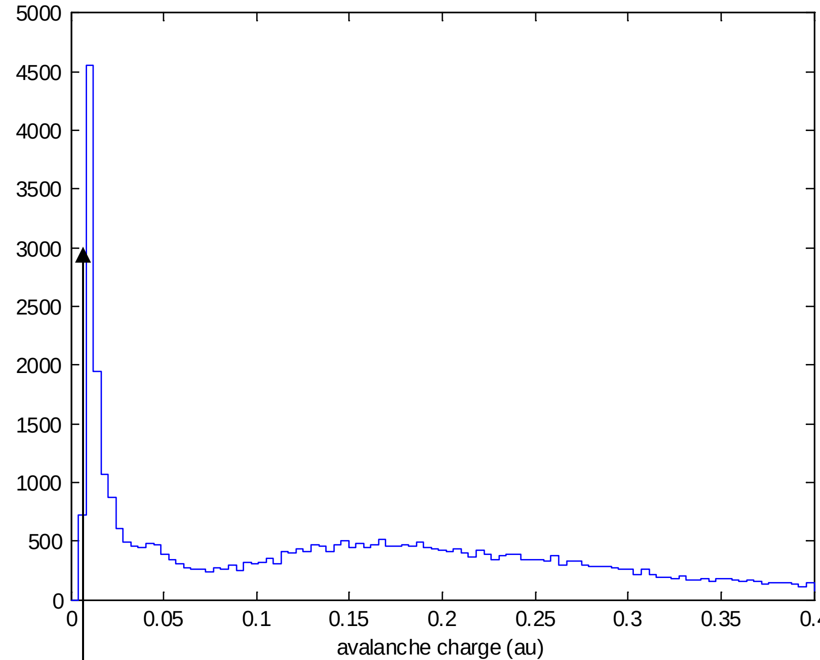

Charge distribution with time trigger

Obviously sub-millimetric resolution
Some systematic deviations
(integral non-linearity)

Note the very low cut fundamental for good efficiency

[Patent pending]

Readout electronics (for both PETs)

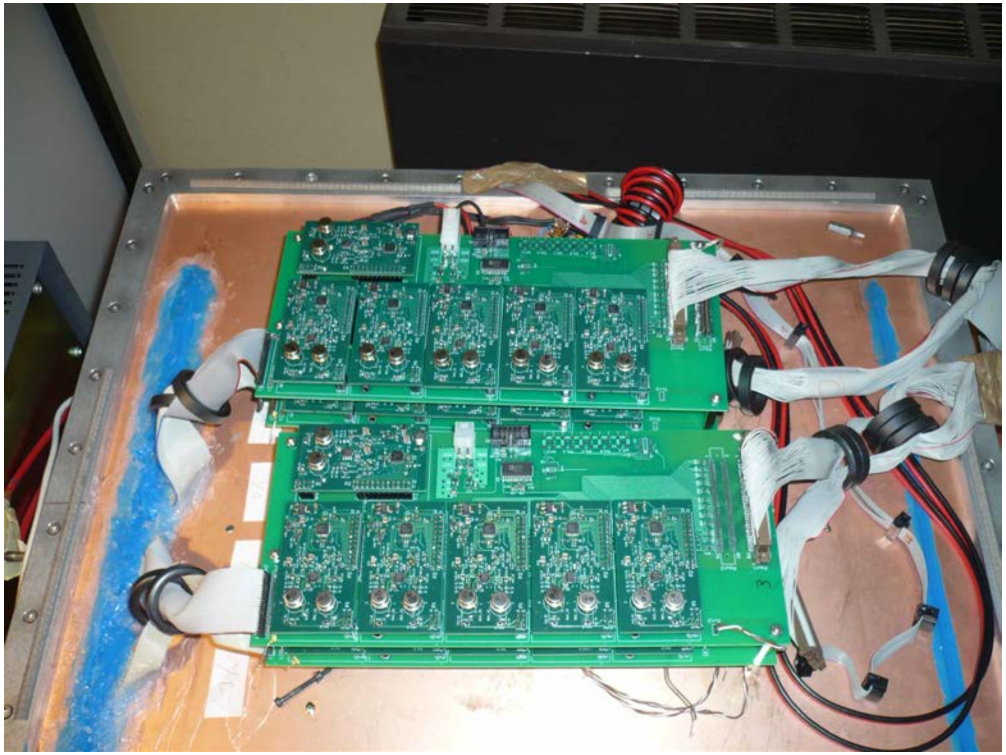

24 channel charge amplifier boards, optimized for large input capacitance.

Each coordinate of each animal PET head needs one such board -> 192 channels

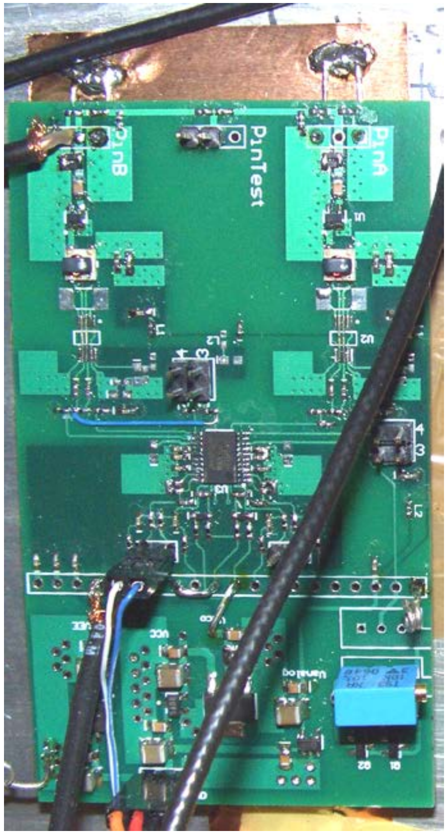

Timing electronics
2 channels @ 3 cm pitch
2 amps + dual discriminator
GHz bandwidth
output: LVDS + analog sum
accuracy ~few tens of ps

Data acquisition system

The HADES experiment at GSI, Germany

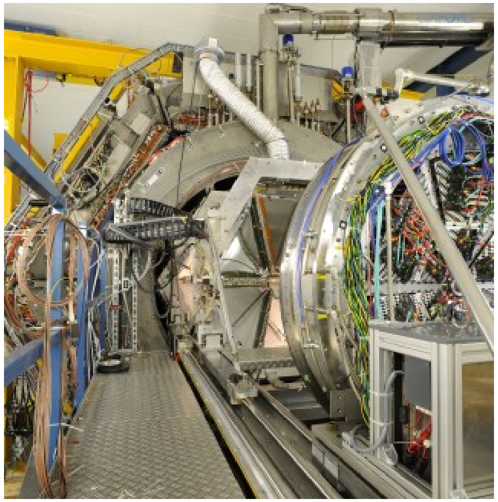

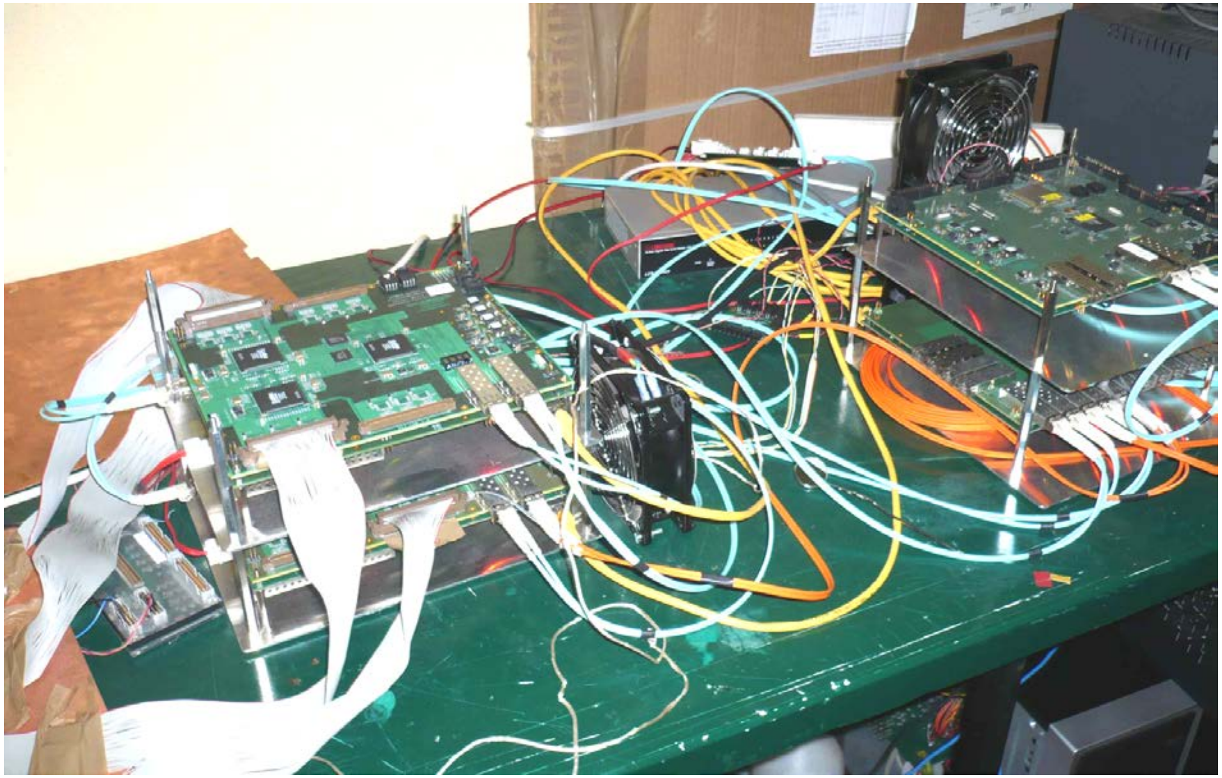

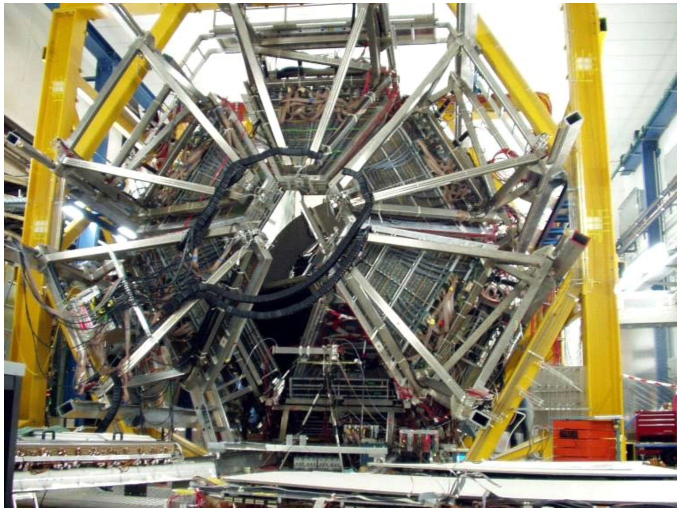

192 channels streaming ADC with Pulse Processing
256 channels multihit TDC
Multihost support

Provided by the HADES DAQ group @ GSI, IKF (Germany) and JU (Poland).

Human PET data chain concept

Multihost support

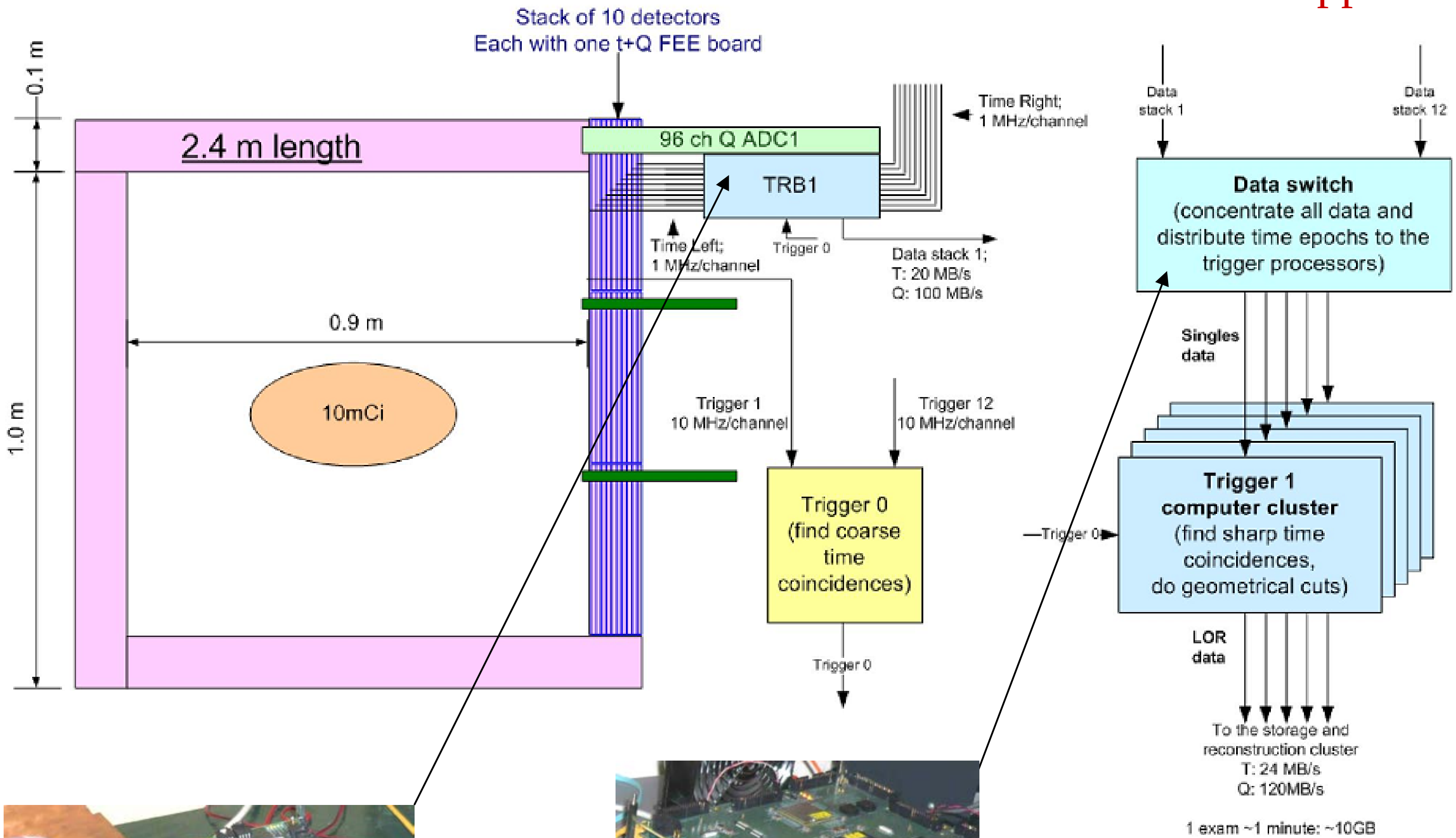

Reconstruction studies - Direct Time-of-Flight Whole Body 3D

NCAT Simulation (whole body)

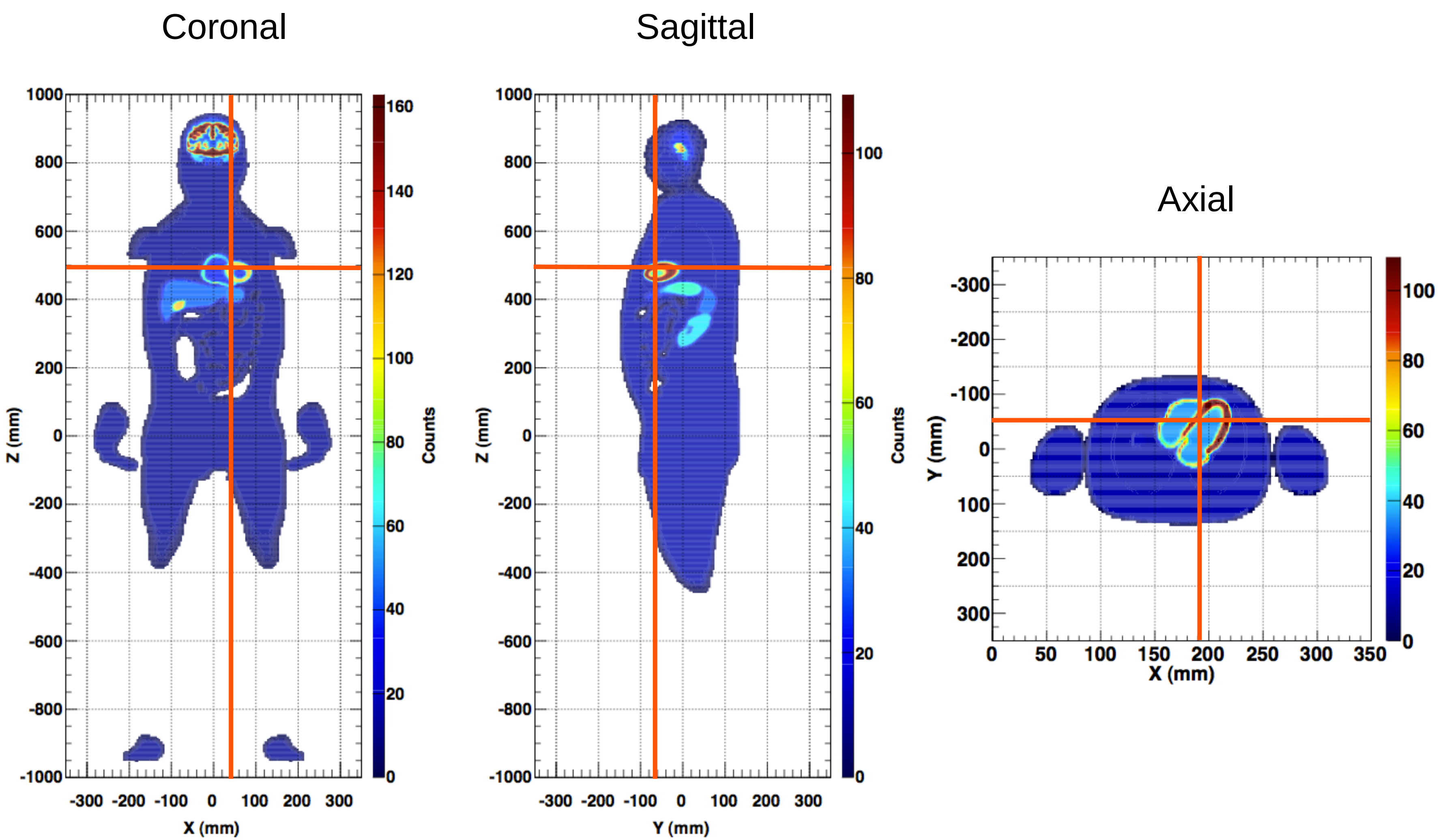

[P.Martins et al., IEEE MIC 2011]

Reconstruction studies - Direct Time-of-Flight Whole Body 3D

Backprojected Image (300 ps FHWM kernel)

Image quality suggests potential real-time imaging capability of RPC-PET

Coronal

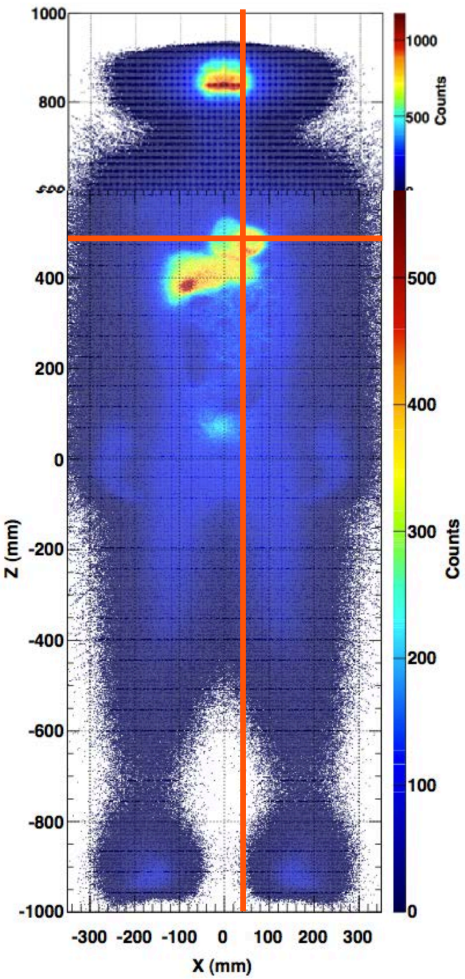

Sagittal

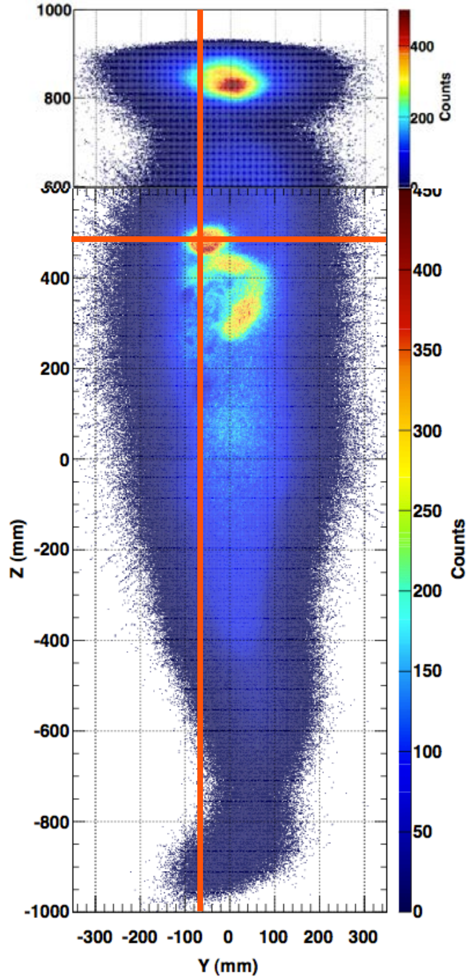

Axial

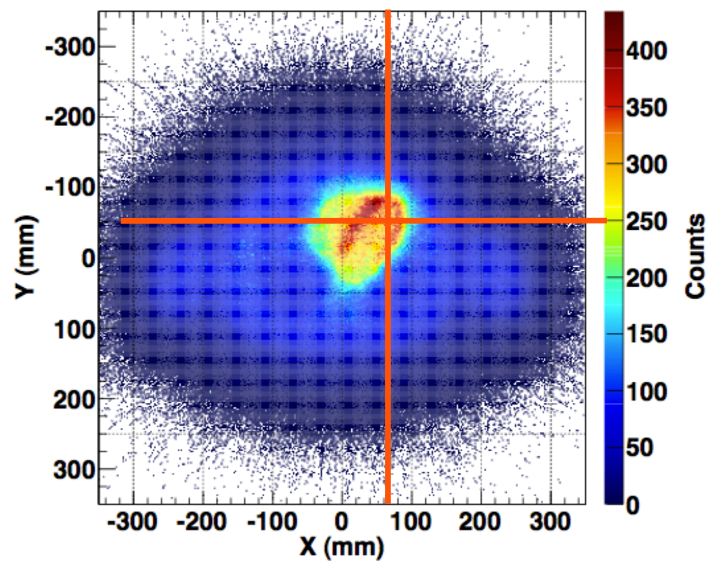

[P.Martins et al., IEEE MIC 2011]

Reconstruction studies - Direct Time-of-Flight Whole Body 3D

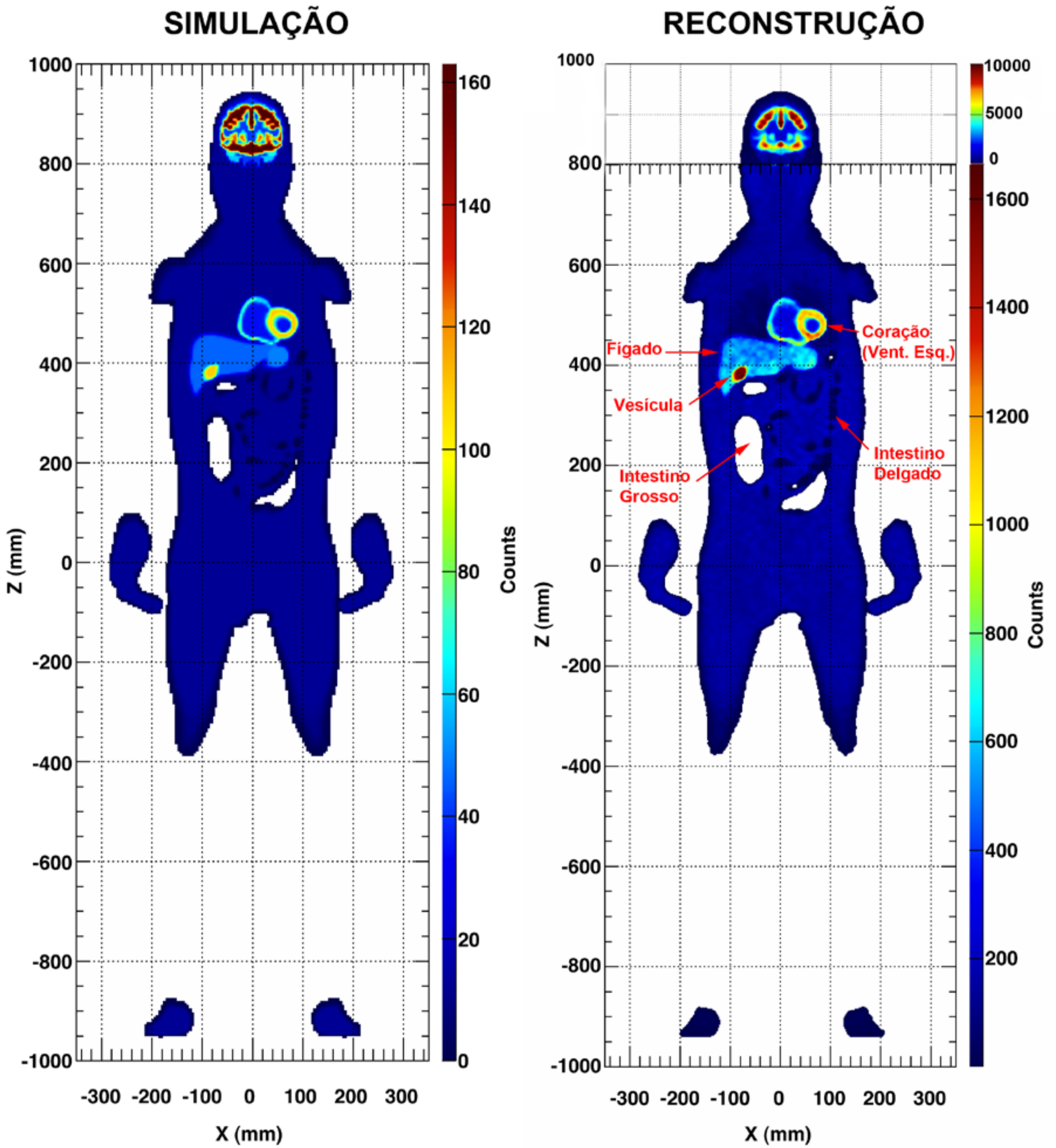

MLEM – 45 iterations

[P.Martins et al., IEEE MIC 2011]

Reconstruction studies - Direct Time-of-Flight Whole Body 3D

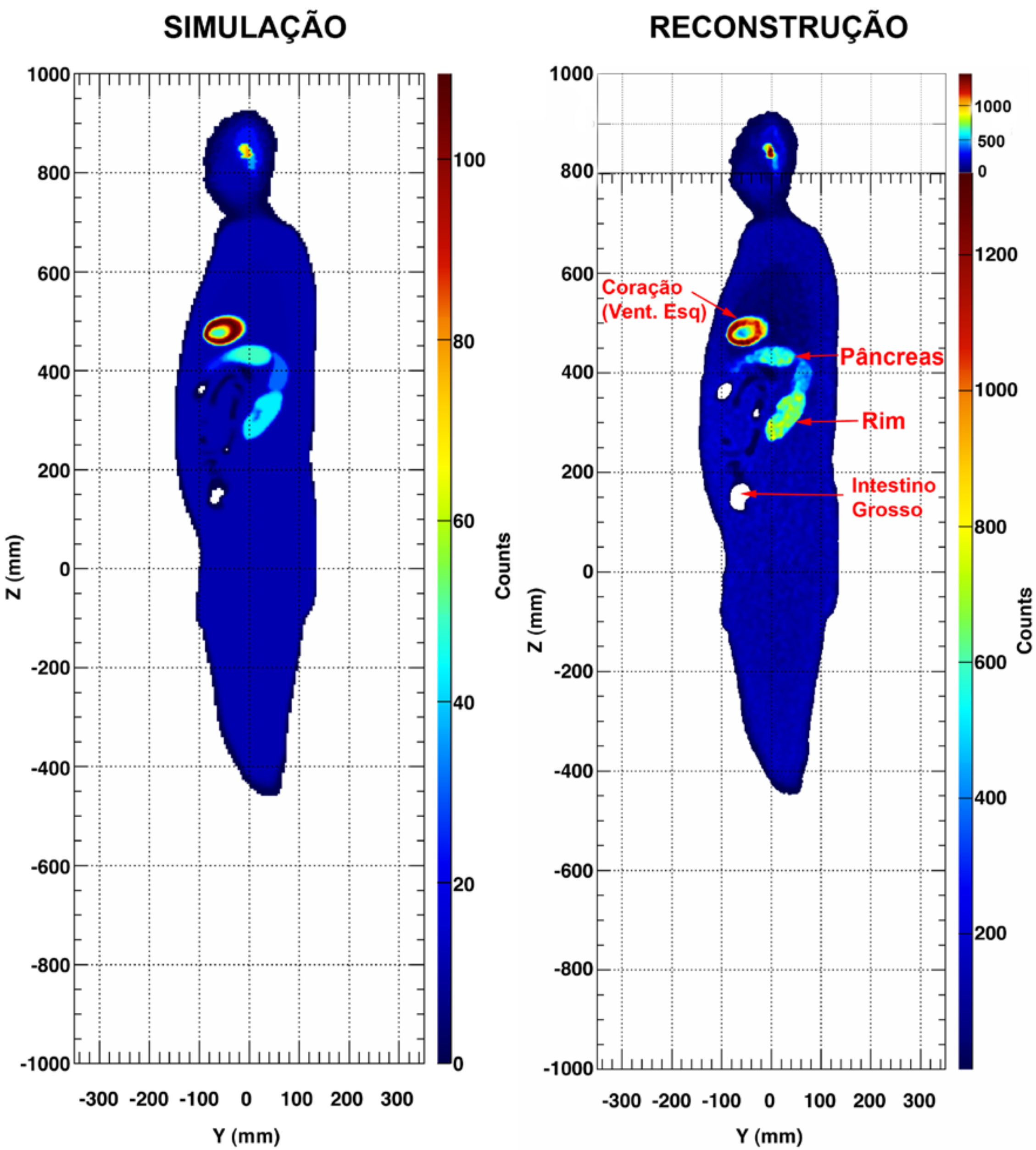

MLEM – 45 iterations

[P.Martins et al., IEEE MIC 2011]

Reconstruction studies - Direct Time-of-Flight Whole Body 3D

MLEM – 45 iterations

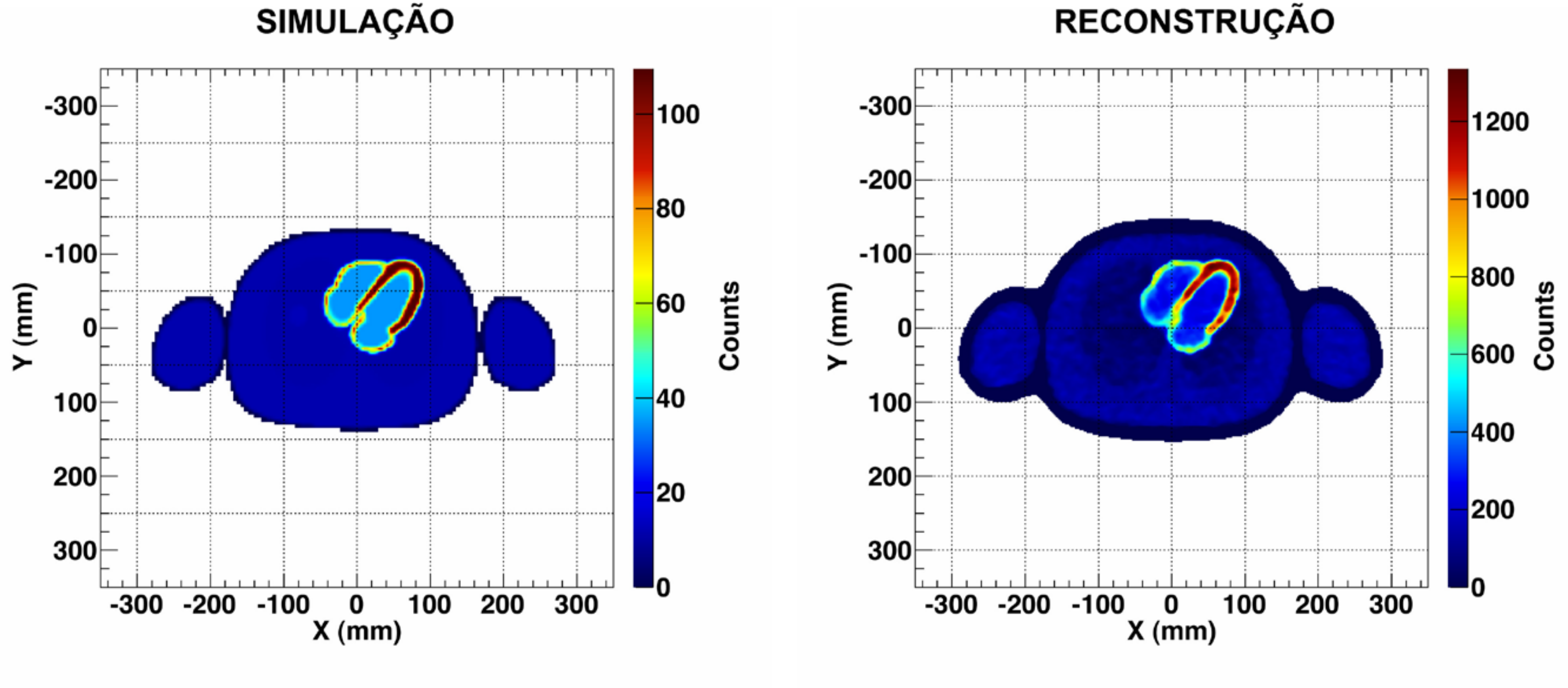

[P.Martins et al., IEEE MIC 2011]

Conclusion

- Innovative RPC applications to PET seem possible in:
  - Whole-body single-bed human TOF-PET, offering **factors 5 to 11 NECR advantage over GEMINI TF (depending on electronics dead time)** without (hopefully) extra cost and excellent position resolution
    - **Comprehensive study in progress**
      - **Full NEMA NU2-2001 simulation finished**
      - **3D whole body MLEM reconstruction demonstrated**
    - **1st full-size prototype (with low efficiency) in development**
      - **Many components developed and tested**
  - High resolution small-animal PET
    - Simulations suggest that a **competitive peak NEC of 318 Kcps** may be obtained for a optimized system dedicated to small animal PET
    - **Full system for mice in construction**
      - **0.4 mm resolution demonstrated in fully realistic geometry, including DOI resolution**